SHIPS AND OFFSHORE STRUCTURES
https://doi.org/10.1080/17445302.2021.1937796

Taylor & Francis
Taylor & Francis Group

An adaptable algorithm to predict the load-shortening curves of stiffened panels in compression

Shen Li*, Do Kyun Kim and Simon Benson

Group of Marine, Offshore and Subsea Technology, School of Engineering, Newcastle University, Newcastle upon Tyne, UK

ABSTRACT

An adaptable algorithm is proposed in this study, which can predict the complete load-shortening curve of a stiffened panel subjected to uniaxial longitudinal compression. The algorithm provides an extension to existing empirical formulae initially derived for predicting the ultimate compressive strength of stiffened panels. Based on observations from a series of nonlinear finite element analyses, the compressive load-shortening behaviour of stiffened panels is idealised with a linear pre-collapse response, an arc-shaped nonlinear ultimate collapse region and an asymptotic post-collapse decay. The algorithm allows direct modification of the elastic stiffness, ultimate strain, ultimate strength and post-collapse characteristics of the load shortening curve. This enables the load shortening curve to incorporate characteristics specific to the type of stiffened panel under analysis. The capability of the algorithm is demonstrated through an application with the simplified progressive collapse method to calculate the ultimate ship hull strength of four merchant ships and one naval vessel.

ARTICLE HISTORY
Received 12 October 2020
Accepted 26 May 2021

KEYWORDS
Ultimate strength; buckling; load-shortening curves; ships and offshore structures; empirical formulation

1. Introduction

Predicting the ultimate strength and progressive collapse behaviour of stiffened panels is critical for local strength assessment of ship structures and is incorporated into most classification rules and safety standards. Furthermore, the load shortening curves of stiffened panels form the input data to evaluate the global collapse behaviour of a ship hull girder using established approaches such as the simplified progressive collapse method (Li et al. 2020a). Many approaches have been proposed to predict the ultimate compressive strength and load-shortening behaviour of stiffened panels. Generally, these can be separated into three distinct types: analytical approaches, numerical methods and empirical formulations. Whilst analytical approaches and numerical methods can usually predict the load-shortening curve in the entire strain range required for collapse analysis, empirical methods are usually restricted to a prediction of the ultimate strength or the ultimate strain.

In this study an advanced algorithm is proposed to develop a complete load shortening curve from four specific characteristics: the elastic stiffness, ultimate strength, ultimate strain and post-collapse response. The ultimate strength is predicted by established empirical formulae, whilst this paper proposes algorithmic approaches to predict the other characteristics based on computational analysis using the nonlinear finite element method (NLFEM). The algorithm extends the usage of these empirical formulae to assess global hull girder strength, for example enabling them to be incorporated directly in the simplified progressive collapse method. Followed by a background section reviewing the state-of-the-art research, the development of the proposed algorithm will be described and then its application is presented.

2. Background

This section provides a selective overview of the various approaches that have been developed to predict the ultimate strength of ship type plates and stiffened panels. The purpose of this section is to demonstrate the breadth of approaches that are available and the methods from which the algorithm developed in this paper will extend.

Analytical approaches are typically developed from the elastic large deflection analysis (Paik et al. 2001a, 2012), effective width concept (Paik et al. 1999) and plasticity mechanism. Dow and Smith (1986) introduced an analytical method to predict the ultimate strength and post-ultimate strength behaviour of a beam-column model. A finite element procedure was employed to solve the force-displacement equation where the stiffener was discretised into a set of fibres and the attached plate was treated as a single element with pre-defined stress/strain response. A similar beam-column model was adopted by Yao and Nikolov (1991, 1992). A series of prescribed stress distributions of the beam-column cross section were established considering large deflection and plastic deformation. The effectiveness of the attached plate was evaluated based on a combination of elastic large deflection analysis and rigid plastic mechanism analysis. Based on the large deflection orthotropic plate approach by Paik et al. (2001b), an adapted large deflection orthotropic plate methodology was proposed by Benson et al. (2015), with a capability to account for both inter-frame and multi-frame buckling collapse modes of an orthogonal stiffened panel. Faulkner et al. (1973) developed an analytical approach considering local plate buckling failure, flexural column buckling and stiffener tripping. The effective width concept (Faulkner 1975) was implemented to consider the loss of effectiveness of local plating caused by buckling. This approach was further extended by Gordo and Guedes Soares (1996) to predict the load-shortening curves of stiffened panels. A highly accessible approach is available in the Common Structural Rules (IACS 2020). The CSR method is established in a similar way to the approach of Gordo and Guedes Soares, but embedded with the Frankland formula (Frankland 1940) to consider the loss of effectiveness caused by buckling using an effective width concept. Meanwhile, the local buckling of stiffener web is also accounted for in

CONTACT Shen Li s.li37@newcastle.ac.uk, shen.li@strath.ac.uk; Do Kyun Kim do.kim@newcastle.ac.uk; Simon Benson simon.benson@newcastle.ac.uk
Group of Marine, Offshore and Subsea Technology, School of Engineering, Newcastle University, Newcastle upon Tyne NE1 7RU, UK
*Present address: Department of Naval Architecture,Ocean and Marine Engineering, University of Strathclyde, Glasgow, UK

the CSR method. Analytical methods may also refer to the development of elements in the Idealised Structural Unit Method (ISUM) with an intention to reduce the degree of freedom and computational time involved in the conventional finite element method. Ueda and Rashed (1984) proposed the first beam-column ISUM element for the collapse analysis of the transverse frame. Similar concepts were employed to develop the plate and stiffened panel ISUM elements (Ueda et al. 1984). An introduction to the Idealised Structural Unit Method and its application is given by Paik and Thayamballi (2003).

Numerical methods, usually based on the nonlinear finite element method (NLFEM), are widely used to investigate the buckling and post-buckling behaviour of stiffened panels under compression. The use of NLFEM enables the evaluation of various parameters of influence, including initial imperfections, secondary loadings, in-service degradations and different materials. There are many papers which include NLFEM analyses of ship-type plates and stiffened panels, only a selection of relevant studies are presented here. An introduction to NLFEM and approaches for marine structures is given by Benson and Collette (2017). Dow and Smith (1984) employed NLFEM to analyse the effects of localised imperfection on the compressive strength of rectangular long plates. Gordo (2015) analysed the influence of initial imperfection on the strength of restrained plating with the aid of finite element analysis. Benson et al. (2011, 2013a) investigated the ultimate strength and load-shortening characteristics of marine-grade aluminium alloy plates in compression. Syrigou and Dow (2018) analysed the collapse behaviour of steel and aluminium plates under combined compression/tension and shear. Li et al. (2019) conducted a parametric finite element analysis to study the structural response of steel plating under cyclic compression and tension. Paik et al. (1998) investigated the stiffener tripping by applying nonlinear finite element analysis. Paik and Seo (2009a, 2009b) discussed the modelling techniques and practical procedure for ultimate strength analysis of plate and stiffened panels under combined biaxial compression and lateral pressure. Recently, the influence of welding residual stress on the ultimate strength of stiffened panels was investigated by Li et al. (2021a) using NLFEM.

NLFEM is now established as a capable method to evaluate the elastoplastic buckling and ultimate strength of ship structures. However, the modelling effort and computational time of finite element methods are substantial compared with other approaches. In addition, as demonstrated by several ISSC benchmark studies (ISSC 2000, 2012; Ringsberg et al. 2021), the finite element solutions may considerably differ because of the uncertainty in modelling techniques, parameter setting and finite element solvers.

Empirical formulations, which can provide a fast and straightforward 'first-cut' estimation of ultimate strength, have also seen continuing development. Lin (1985) proposed a simple expression in terms of the plate slenderness ratio and column slenderness ratio to estimate the ultimate compressive strength of stiffened panels. Linear regression analysis was utilised to determine the empirical constants based on experimental data. The empirical constants were modified by Paik and Thayamballi (1997) with additional experimental data to improve the accuracy for predicting the ultimate strength of stiffened panels with higher column slenderness ratios. Empirical formulations were also developed in the form of design charts (Chalmers 1993) where the ultimate compressive strength of stiffened panels was given as a function of plate slenderness, column slenderness and cross section area ratio. Recently, empirical formulae were introduced by Zhang and Khan (2009) and Kim et al. (2017) based on finite element results. Empirical formulations are usually developed as a simple expression. However, Kim et al. (2018a) stressed that the simple expression (= single line approach based on the plate and column slenderness ratios) may be inadequate to estimate the ultimate strength of stiffened panels, especially for those with small column slenderness ratios (= stocky and intermidinate columns). To this end, Kim et al. (2019, 2020) proposed refined empirical formulations through data processing for T-bar and flat bar stiffened panels and introduced novel dimensionless parameters (h_w/t_w and I_{pz}/I_{sz}), in which an improved accuracy was shown.

As illustrated by the schematic overview in Figure 1, both analytical approaches and numerical methods can predict the ultimate strength and post-ultimate strength behaviour, whereas the empirical formulation is limited to the prediction of structural capacity at the ultimate limit state (ULS). Although the former is relatively well established, the empirical methods are still highly useful, since only a few basic scantling parameters and simple calculation procedures are required. Therefore, to extend the capability of existing empirical formulae, an adaptable algorithm to predict the compressive load-shortening curve over the full strain range required for progressive collapse analysis is proposed in this paper. The proposed formulation allows for a convenient modification of the elastic stiffness, ultimate strain, ultimate strength and post-ultimate characteristics of stiffened panels in longitudinal compression. To demonstrate the capability of the empirical formulation, a case study incorporating with the simplified progressive collapse method is conducted to predict the ultimate ship hull strength of four merchant vessels and one naval ship.

3. Evaluation of existing empirical methods

A number of empirical methods are proposed to predict the ultimate strength of stiffened panels under compression. This section evaluates the performance of four existing empirical methods: Paik and Thayamballi formula (1997), Zhang and Khan formula (2009), Kim et al. formula (2017) and column collapse strength design chart (Chalmers 1993) developed by the Admiralty Research Establishment (A.R.E.). Equations (1) to (3) and Figure 2 give the formulations of all these methods. A comprehensive technical review on this subject may also refer to Kim et al. (2018a) where a statistical comparison was made for empirical formulations on the ultimate strength prediction of a wide spectrum of stiffened panels. This section aims to provide an evaluation on different sub-domains covering a smaller range.

Paik and Thayamballi formula (P – T)

$$\frac{\sigma_{xu}}{\sigma_{Yeq}} = \frac{1}{\sqrt{0.995 + 0.936\lambda^2 + 0.176\beta^2 + 0.188\lambda^2\beta^2 - 0.067\lambda^4}}$$
$$\beta = \frac{b}{t_p}\sqrt{\frac{\sigma_{Yp}}{E}}$$
$$\lambda = \frac{a}{\pi r}\sqrt{\frac{\sigma_{Yeq}}{E}}$$
$$r = \sqrt{I/A} \tag{1}$$

Zhang and Khan formula (Z – K)

$$\frac{\sigma_{xu}}{\sigma_{Yeq}} = \frac{1}{\beta^{0.28}}\frac{1}{\sqrt{1+\lambda^{3.2}}} \text{ for } \lambda < \sqrt{2} \text{ and } \beta = 1.0 \text{ if } \beta < 1.0 \tag{2}$$

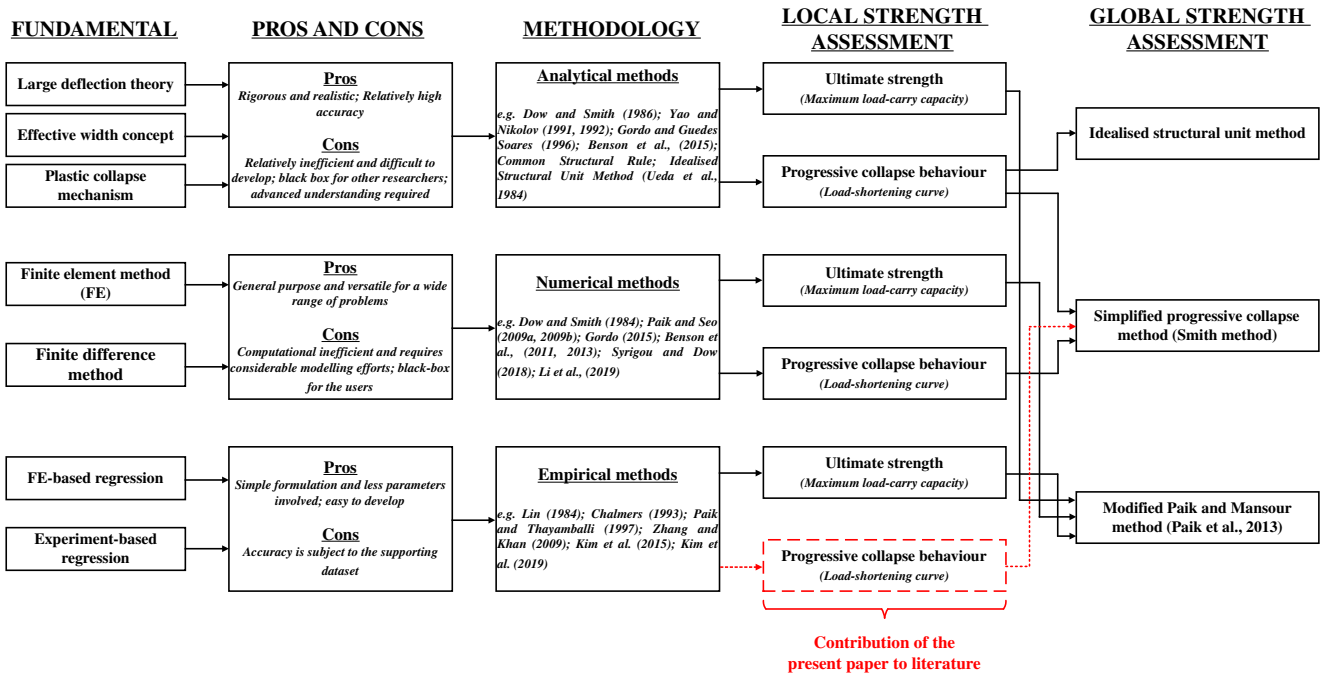

Figure 1. Overview of stiffened panel buckling methods for global strength assessment.

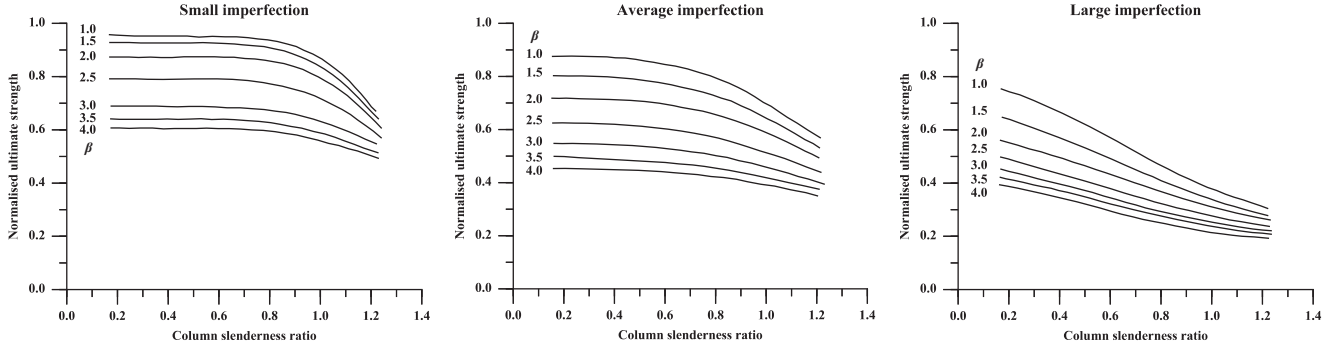

Figure 2. A.R.E. column collapse design charts reproduced from Chalmers (1993).

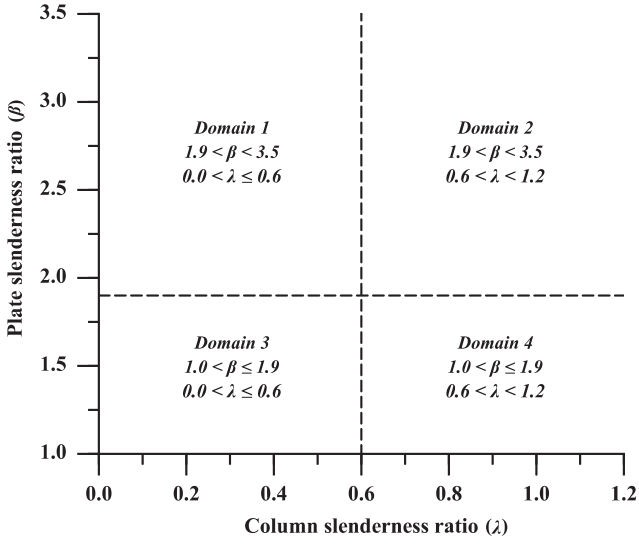

	Domain 1		Domain 2	
	Mean	C.O.V.	Mean	C.O.V.
P-T / Z-K	0.8525	0.0521	0.8665	0.0664
P-T / Kim	0.9375	0.0604	1.0111	0.0784
P-T / A.R.E.	1.0693	0.0443	0.9662	0.0213
Z-K / Kim	1.0996	0.0243	1.1661	0.0184
Z-K / A.R.E.	1.2580	0.0709	1.1203	0.0748
Kim / A.R.E.	1.1461	0.0897	0.9618	0.0873
	Domain 3		Domain 4	
	Mean	C.O.V.	Mean	C.O.V.
P-T / Z-K	0.9189	0.0227	0.9452	0.0483
P-T / Kim	1.0645	0.0157	1.1122	0.0435
P-T / A.R.E.	1.0163	0.0366	0.9537	0.0351
Z-K / Kim	1.1589	0.0230	1.1770	0.0101
Z-K / A.R.E.	1.1056	0.0172	1.0099	0.0252
Kim / A.R.E.	0.9547	0.0348	0.8580	0.0222

*Note: $0.0 < \lambda < 0.6$ Local plate buckling
$0.6 < \lambda < 1.3$ Beam column buckling
$\lambda > 1.3$ Overall buckling

$\beta < 1.9 \quad \sigma_{xu}/\sigma_{Yeq} = 1.0$
$\beta > 1.9 \quad \sigma_{xu}/\sigma_{Yeq} = 1.9/\beta$

Figure 3. Statistical evaluation of the existing empirical formulation.

Kim et al. formula

$$\frac{\sigma_{xu}}{\sigma_{Yeq}} = \frac{1}{0.8884 + \exp(\lambda^2)} + \frac{1}{0.4121 + \exp(\sqrt{\beta})} \quad (3)$$

A statistical evaluation is given in Figure 3 between four empirical methods on the ultimate compressive strength prediction. This evaluation is conducted for different sub-domains. It was suggested by Ozdemir et al. (2018) that the primary failure mode of stiffened panels under compression may change from

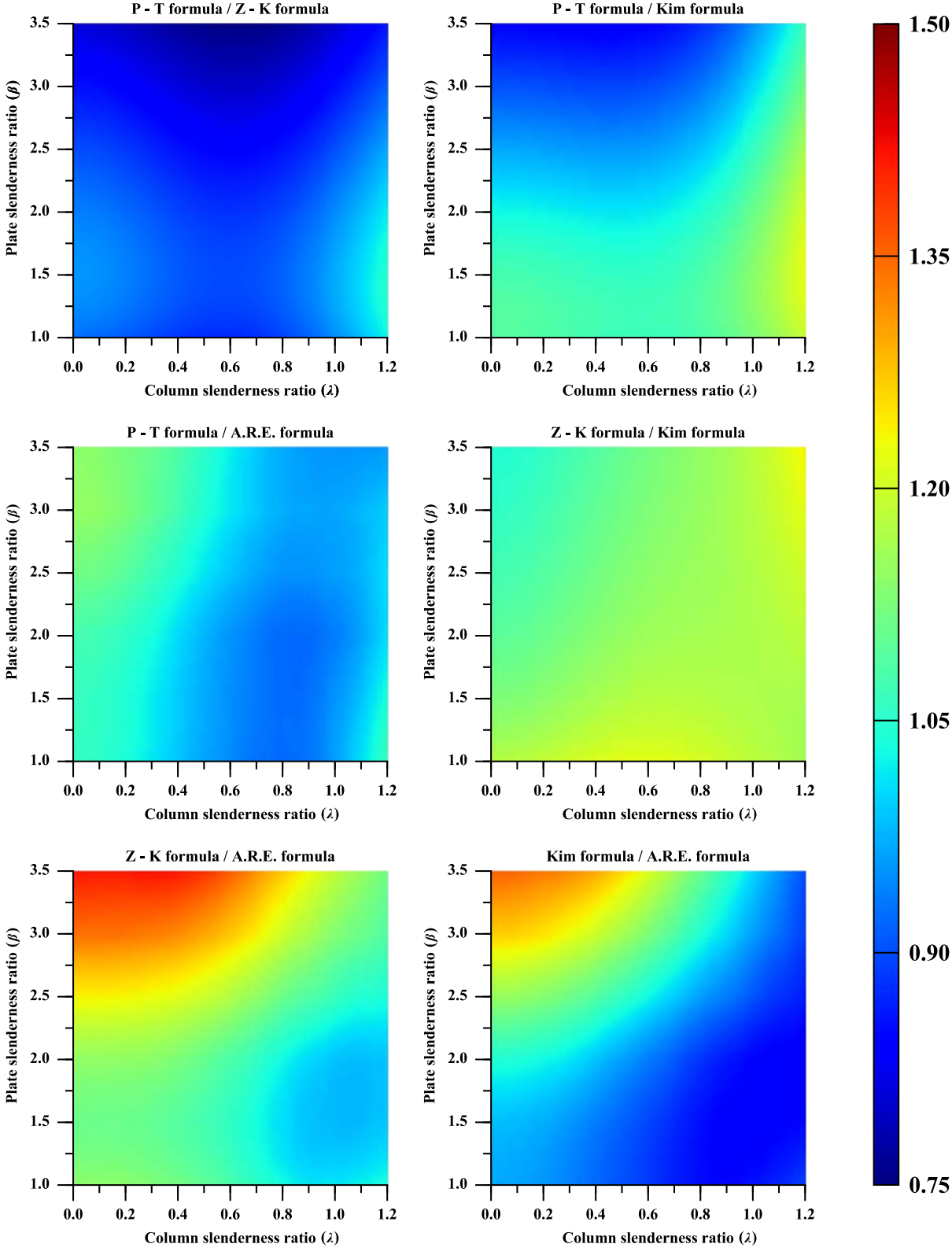

Figure 4. Comparison of the ultimate compressive strength prediction between different empirical methods (This figure is available in colour online).

Table 1. Case study stiffened panel configurations.

	No.	h_w [mm]	t_w [mm]	b_f [mm]	t_f [mm]	σ_{ys} [MPa]	E [MPa]
Stiffener	S1	138	9	90	12	313.6	205800
	S2	235	10	90	15	313.6	205800
	S3	383	12	100	17	313.6	205800
	S4	580	15	150	20	313.6	205800
	No.	a [mm]	b [mm]	t [mm]	σ_{yp} [MPa]	E [MPa]	
Attached plate	P1	2550	850	13 ~ 33	313.6	205800	
	P2	3600	900	14 ~ 35	313.6	205800	
	P3	4750	950	15 ~ 37	313.6	205800	
Plate stiffener combination		P1 + S1	P2 + S2	P3 + S3		Total = (4 + 3 + 2) × 7 = 63	
		P1 + S2	P2 + S3	P3 + S4			
		P1 + S3	P2 + S4				
		P1 + S4					

local plate buckling to beam–column buckling at the threshold $\lambda = 0.6$. On the other hand, the compressive strength of plating may change substantially when $\beta > 1.9$. Hence, four sub-domains are proposed as $\lambda < 0.6$ & $\beta > 1.9$ (Sub-domain 1), $\lambda > 0.6$ & $\beta > 1.9$ (Sub-domain 2), $\lambda < 0.6$ & $\beta < 1.9$ (Sub-domain 3) and $\lambda > 0.6$ & $\beta < 1.9$ (Sub-domain 4). The ratio between ultimate compressive strength prediction is also shown as contour plots in terms of the plate slenderness ratio and column slenderness ratio in Figure 4. Note that linear interpolation is applied to the A.R.E. charts with average imperfection. From these comparisons, the following insights may be developed:

(1) A considerable uncertainty exists between the predictions by different empirical methods. The Z – K formula appears to be the most conservative with respect to other formulae. Notably, Z – K method has a nearly uniform variation with P – T and Kim formulae.
(2) The differences in data acquisition and initial imperfection characteristics may be the most influential parameters affecting the performance of each empirical method. The P – T formula was developed from experimental measurements. Hence, both initial distortion and welding-induced residual stress were implicitly included. Z – K and Kim formulae were proposed on the basis of ABAQUS and ANSYS finite element solutions respectively, both of which excluded the effect of welding-induced residual stress. In addition, the deflection magnitudes were also different. For the local plate deflection, Z – K formula is embedded with the Dowling's recommendation, whereas Kim et al. formula follows Smith's recommendation (Smith et al. 1991), i.e. $w_{\max} = b/200$ and $w_{\max} = 0.1\beta^2 t$ respectively. Chalmers design charts were introduced based on theoretical results obtained from the analytical method developed by Dow and Smith (1986). Both initial deflection and welding-induced residual stress were considered following Smith's recommendation. Also, only the beam-column buckling failure can be simulated.
(3) The differences in regression analysis techniques and the range of datasets may induce further uncertainty. P – T formula was derived using linear regression technique, whereas Z – K and Kim formulae were developed by nonlinear regression. Meanwhile, the dataset for developing P – T and Kim formulae covered stiffened panels with very high column slenderness ratio. By contrast, Z – K formula and Chalmers design charts only covered stiffened panels with low and moderate column slenderness ratio. Hence, the bias toward the slender stiffened panels may offset the data collected from stocky stiffened panels and thereby illustrate a conservative prediction for the present comparison.

4. Numerical investigation using NLFEM

To provide the development basis of the adaptable algorithm, a series of numerical analyses using NLFEM are conducted on stiffened panels with representative ship structural scantlings (Table 1). The observations and insights developed from the results of finite element analyses will be used for the idealisation of the compressive load-shortening behaviour of stiffened panels. For the attached plates, three aspect ratios and seven slenderness ratios are examined ($a/b = 3.0$, 4.0 and 5.0; $\beta = 1.0 \sim 2.5$). For $a/b = 3.0$, four stiffener sizes are analysed (S1, S2, S3 and S4). For $a/b = 4.0$, three stiffener sizes are tested (S2, S3 and S4). For $a/b = 5.0$, two stiffener sizes are investigated (S3 and S4). A total of 63 stiffened panels are selected for finite element (FE) analysis. The distribution of the resulting column slenderness ratio of the stiffened panels used in this study for FE analysis is shown in Figure 5. The column slenderness ratios are varied from 0.1 to 0.9 and primarily centred at 0.1–0.5, which is a typical configuration of ship-type stiffened panels according to Zhang and Khan (2009). The material yield stress and Young's modulus of all panels are 313.6 and 205,800 MPa respectively. In this study, we adopted the same stiffened panel scenarios from ISSC (2012). The probability density distributions for the local elements, i.e., stiffened panel and unstiffened panel, may be referred to Kim et al. (2017, 2018b), respectively. An elastic-perfectly plastic material behaviour is assumed. The material hardening has been shown to have minimal effect on the pre-collapse response and the ultimate compressive strength of structural members (Li et al. 2019). The post-collapse response would

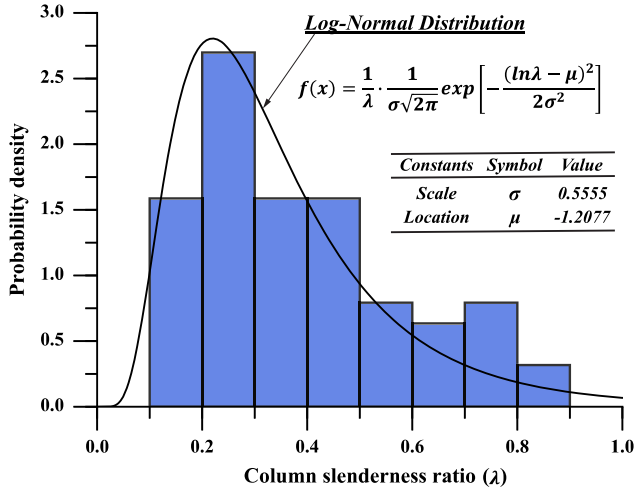

Figure 5. Probability density of the column slenderness ratio of the selected stiffened panels for analysis (This figure is available in colour online).

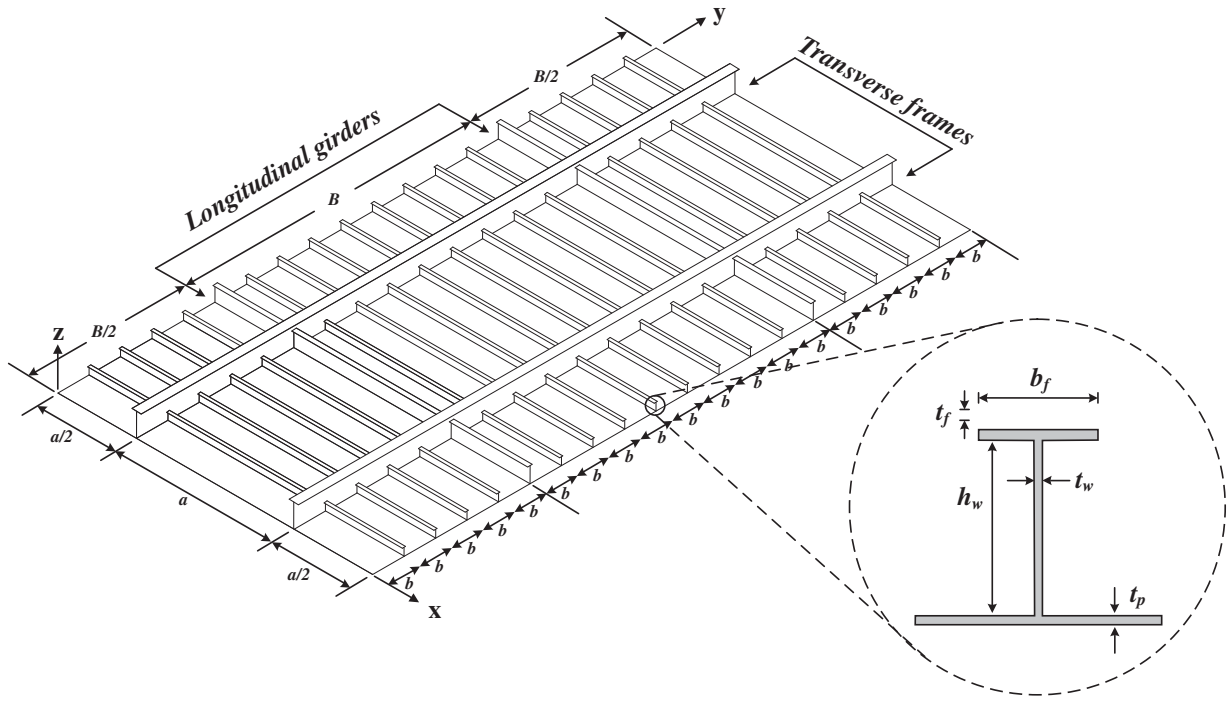

Figure 6. Illustration of a typical stiffened panel of ship structures.

generally follow the same response pattern but a smaller decay rate. However, this change should be subject to the hardening modulus of the material. The justification of assuming an elastic-perfectly plastic material behaviour usually is that when the hull girder attains its ultimate strength, the most critical structural component normally will not far exceed its own ultimate limit state. Even for the very slender structures such as warship cross section, it is usually less than $2.0\varepsilon_x/\varepsilon_{Yeq}$ as indicated by Smith (1977). In addition, the bilinear elastic-perfectly plastic stress–strain curve produces less uncertainties as compared to a detailed material curve. Hence, this paper follows the common practice in ultimate limit state assessment where the material behaviour is assumed as elastic-perfectly plastic which is widely used and highlighted by ISSC reports (2012).

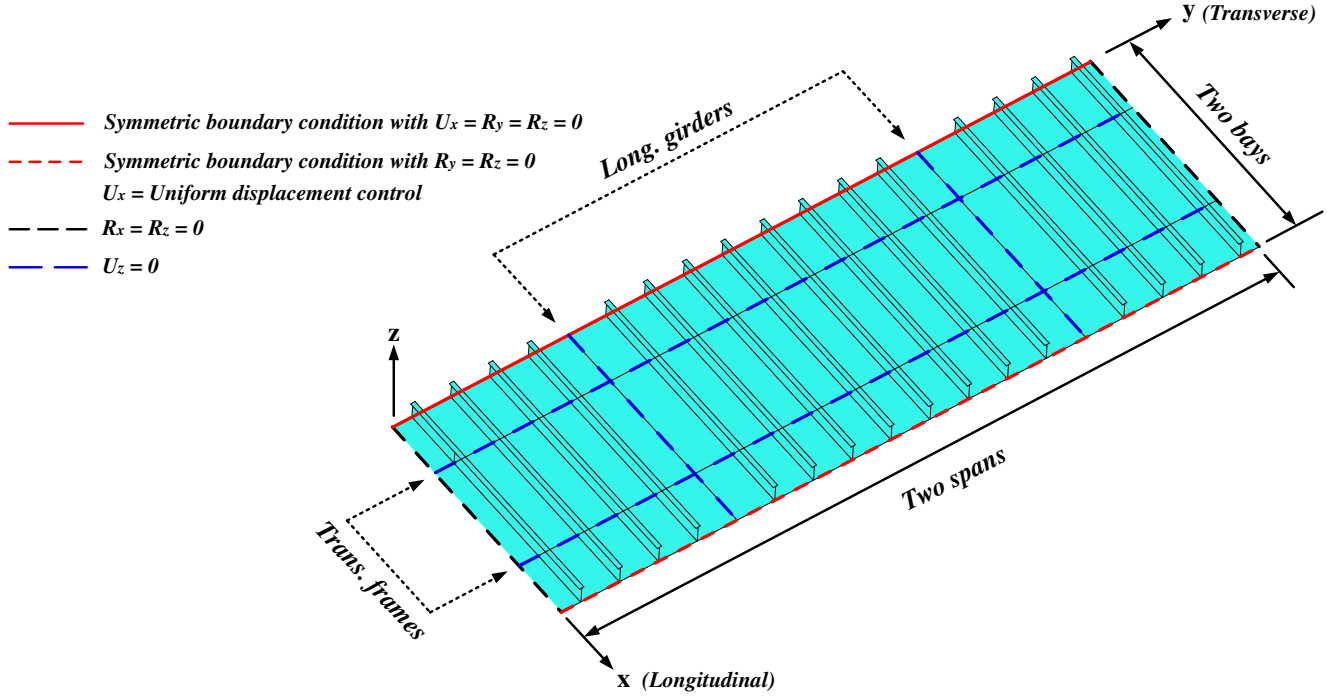

Figure 7. The boundary conditions of the FE model (This figure is available in colour online).

4.1. Finite element modelling

A typical ship's stiffened panel with definition of all relevant parameters is shown in Figure 6. It was discussed by ISSC (2012) that the constraint of the end-rotation of stiffeners may over-estimate the ultimate compressive strength of stiffened panels. Meanwhile, Smith et al. (1991) indicated the interaction between longitudinal adjacent structures should be considered. Hence, a two-span/two-bay model with eight identical stiffeners at each span is employed in the present study (Figure 7). The present model extent is valid for stiffened panels with identical stiffeners over a relatively large transverse span, such as the primary deck panels. However at the bottom panels of a ship, the number of stiffeners within each span could be different from that at the deck, in which case the load-shortening behaviour may substantially differ from the prediction based on the model extent adopted in this study. Nevertheless, as shown by Tanaka et al. (2014), this uncertainty would not be significant for conventional configurations of ship structures. The longitudinal girders and transverse frames are modelled with boundary conditions constraining the out-of-plane movement. The present model extent and applied boundary conditions are consistent with the ISSC (2012) and Kim et al. (2017), which allow for the end-rotation of stiffeners and the interactions between the adjacent structures in the longitudinal direction and may be a reasonable representation of typical ship structures. The effect of different boundary conditions on the collapse behaviour of stiffened panel could refer to Xu et al. (2013). The attached plating is discretised by $10\times a/b$ and 10 elements in longitudinal and transverse directions respectively. Six elements are used for discretising the web and the flange of the stiffeners. The loaded edges are kept straight by employing a reference point for load application and the compressive load is applied through displacement control.

The scope of this study is confined to the load-shortening characteristics of stiffened panels with uniform thickness under uniform monotonic compression in an ordinary operational environment. The influence of non-uniform thickness of the panel and non-uniform compression were studies by Anyfantis (2020) and Lee and Paik (2020) respectively. The former could occur in the transitional area with varying thicknesses and the latter could be found on the side shell panels. The ULS assessment of stiffened panels in exceptional conditions such as artic environment and elevated temperature may refer to the recent works by Paik et al. (2020a, 2020c) and Fanourgakis and Samuelides (2021) respectively. The load-shortening behaviour of stiffened panels under cyclic axial load, which could occur in a series of storm waves, was investigated by Paik et al. (2020b) and Li et al. (2019). In addition, apart from a direct analysis on stiffened panels, a new procedure to develop the load-shortening curve of structural components was discussed by Downes et al. (2017). This approach utilises the load-shortening data extracted from the numerical simulation of simple box-girder under vertical bending. With this approach, more realistic boundary conditions of stiffened panel elements can be considered, such as the interaction between the deck panels and side shell panels, which is not able to be evaluated by the present modelling approach. A future benchmark study could be performed to compare the load-shortening curves obtained from direct analysis on stiffened panels and extracted from box girder test.

The initial imperfection is applied using a direct node translation technique (Benson et al. 2012). As shown in Figure 8, three types of deflection modes are considered, namely local plate initial deflection w_{opl}, column-type initial deflection w_{oc} and stiffener sideway initial deflection w_{os} (Equations (4)–(6)). The shape of the local plate distortion is a combination of 80% of single half sine wave, 20% of a critical buckling mode half sine waves and 1% of a high-order mode. The first two modes represent a realistic distortion of critical buckling, while the high-order mode ensures that the nucleation of out-of-plane deflection occurs at one part of the plate. The magnitudes of each deflection are determined by Equations (7) to (9). Residual stress is not considered in the present analysis. An illustration of the FE model with initial distortion is shown in Figure 9.

$$w_{opl}=A_o\left\{0.8\sin\left(\frac{\pi x}{a}\right)+0.2\sin\left(\frac{m\pi x}{a}\right)+0.01\sin\left[\frac{(m+1)\pi x}{a}\right]\right\}\sin\left(\frac{\pi y}{b}\right)$$
$$m=a/b+1 \tag{4}$$

$$w_{oc}=B_o\sin\left(\frac{\pi x}{a}\right)\sin\left(\frac{\pi y}{B}\right) \tag{5}$$

$$w_{os}=C_o\frac{z}{h_w}\left[0.8\sin\left(\frac{\pi x}{a}\right)+0.2\sin\left(\frac{i\pi x}{a}\right)\right]$$
$$i=a/h_w+1 \tag{6}$$

$$A_o=0.1\beta^2 t \tag{7}$$

$$B_o=0.0015a \tag{8}$$

$$C_o=0.0015a \tag{9}$$

4.2. Results and discussions

A comparison of the ultimate compressive strength prediction by the present numerical analysis and four empirical formulae is shown in Figure 10. Overall, the validity of the NLFEM analysis results is confirmed. The statistical analysis shows the closest correlation is obtained with Z–K formula, which was also developed by ABAQUS FE results. The present FE overpredicts the ultimate strength when compared with the other formulae. This may be due to the uncertainty of imperfections and differences in FE solver. In addition, it should be noted that the numbers of stiffened panels at each sub-domain are not the same, which may have an implication in the interpretation of the statistical comparison.

Further validation is completed by a comparison of load-shortening curves with the benchmark study of ISSC (2012), given in Figure 11. This attempts to replicate the ISSC benchmark simulations by adopting the same model extent and imperfection characteristics. A close correlation is shown on the one bay/one span model, whereas a higher ultimate compressive strength is predicted on the two bay/two span model. This may be attributed to the difference in FE solver and the formulation of shell element, since ANSYS was employed in the ISSC benchmark.

A prediction based on the modelling technique outlined in Section 4.1 (ABAQUS solver and A.R.E. imperfection) is also presented in Figure 11. This shows a higher initial stiffness and steeper post-collapse response, while the ultimate compressive strength is reasonably correlated. The difference in initial stiffness may primarily be attributed to the difference in local plate distortion. The present paper follows the A.R.E. recommendation where the local plate distortion is mainly composed by a single half wave and the critical

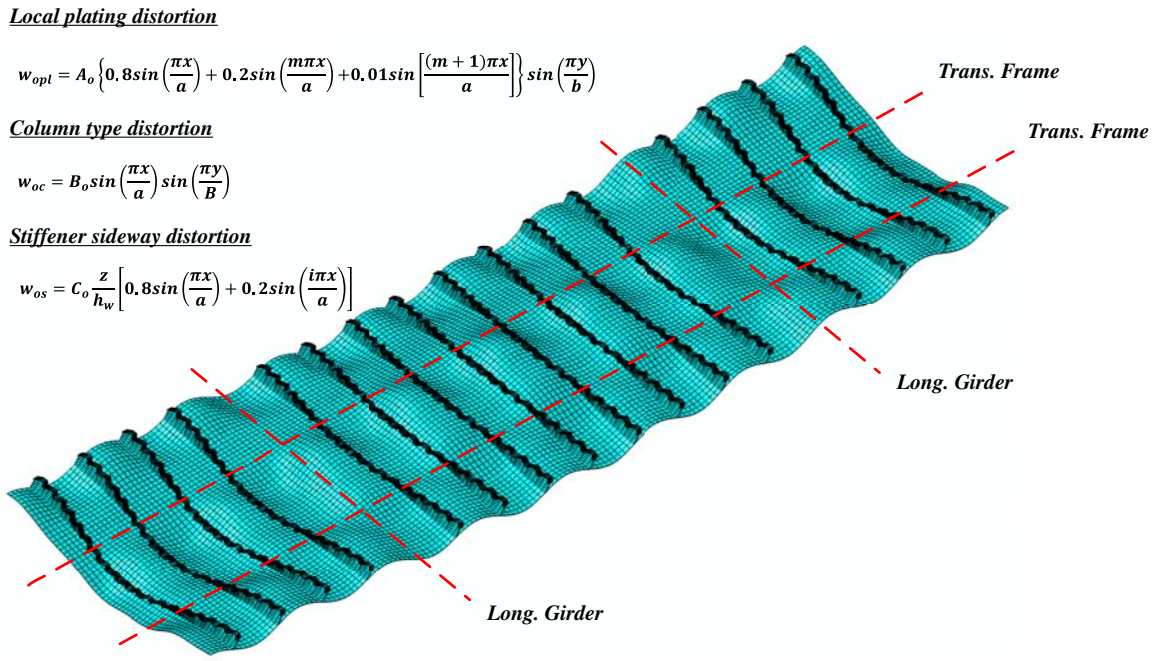

Figure 9. Illustration of NLFEM stiffened panel model with imperfections magnified (This figure is available in colour online).

buckling mode. This may be a simplified way of modelling realistic initial plate distortion as discussed by Benson (2011). Conversely, the ISSC benchmark study only adopted the critical buckling mode. Due to single half wave component, a higher initial stiffness is presented since the critical buckling distortion is prevented. In the post-collapse regime, the distortion nucleation will take place under the A.R.E. imperfection, whereas out-of-plane deflection usually follows the initial shape when only the critical buckling mode is considered. This is consistent with previous findings, for example by Dow and Smith (1984).

The load-shortening curves predicted by NLFEM are shown in Figure 12. From these diagrams, the following observations may be made:

- The pre-ultimate response is predominantly linear elastic. The elastic stiffness of stiffened panels may differ because of the difference in initial imperfection characteristics, such as deflection magnitudes and deflection shapes.
- The onset of plasticity and buckling results in a nonlinear transition from the linear elastic response to the ultimate region, in which the peak represents the ultimate compressive strength of the stiffened panels. The sharpness of this nonlinear transition appears to be primarily governed by the plating thickness of the stiffened panels. A stockier plating leads to sharper nonlinear transition, whereas a more gradual nonlinear transition is seen on slender plating.
- The ultimate strain normalised by the material yield strain deviates from $\varepsilon_{xu}/\varepsilon_{Yeq} = 1.0$, which is the assumption of CSR method. Stiffened panels with higher column slenderness ratio λ would fail at $\varepsilon_u/\varepsilon_y \ll 1.0$, whereas the ultimate strain of stiffened panels with lower slenderness ratio is generally close to unity. This is highlighted in the comparison of load-shortening curves predicted by CSR and NLFEM in Figure 13.
- The post-ultimate regime generally exhibits a drastic drop of strength with a decreasing rate. A significant reduction of post-collapse strength immediate to the collapse is followed by a relatively steady decrease. The post-ultimate strength behaviour is affected by stiffener size and plating aspect ratio. With a smaller stiffener scantling, the post-ultimate range experiences an unstable response. Similar observations can be found in stiffened panels with large aspect ratios.

5. Development of the load shortening curve algorithm

5.1. Proposed adaptable algorithm

The procedure to develop the adaptable algorithm in the present study is illustrated in Figure 14. As seen from the NLFEM case study, a typical compressive load-shortening response of stiffened panels may be idealised as linear elastic initial response, followed by a nonlinear transition to the ultimate strength and asymptotic post-collapse decay. This idealised behaviour is the basis to develop an adaptable algorithm for predicting the load-shortening curves of stiffened panels over a strain range suitable for progressive collapse analysis. The proposed formulation is formed of a linear elastic pre-ultimate response, arc-shaped nonlinear ultimate collapse region and exponential post-ultimate decay. A graphical representation is shown in Figure 15 with all parameters defined by Equations (10)–(15).

Allowance is given in the proposed formulation for a convenient modification of the elastic stiffness, ultimate strain, ultimate strength and post-collapse characteristics. In contrast to the CSR method where the elastic stiffness always equals one, the elastic stiffness of the stiffened panel can be specified as $\bar{E}_{T_o} \leq 1$ depending on the initial imperfection severity. Likewise, the non-dimensional ultimate strain value can be prescribed according to different structural dimensions, as reflected by the present NLFEM numerical analysis. The ultimate compressive strength can be predicted by any available methods, including analytical solution and empirical estimation. An exponential post-collapse response with asymptotic decay is suggested in the present study, in which the empirical coefficients C controls the asymptotic convergence. To illustrate the adaptability of the proposed empirical formulation, a collection of the example load-shortening curves with various

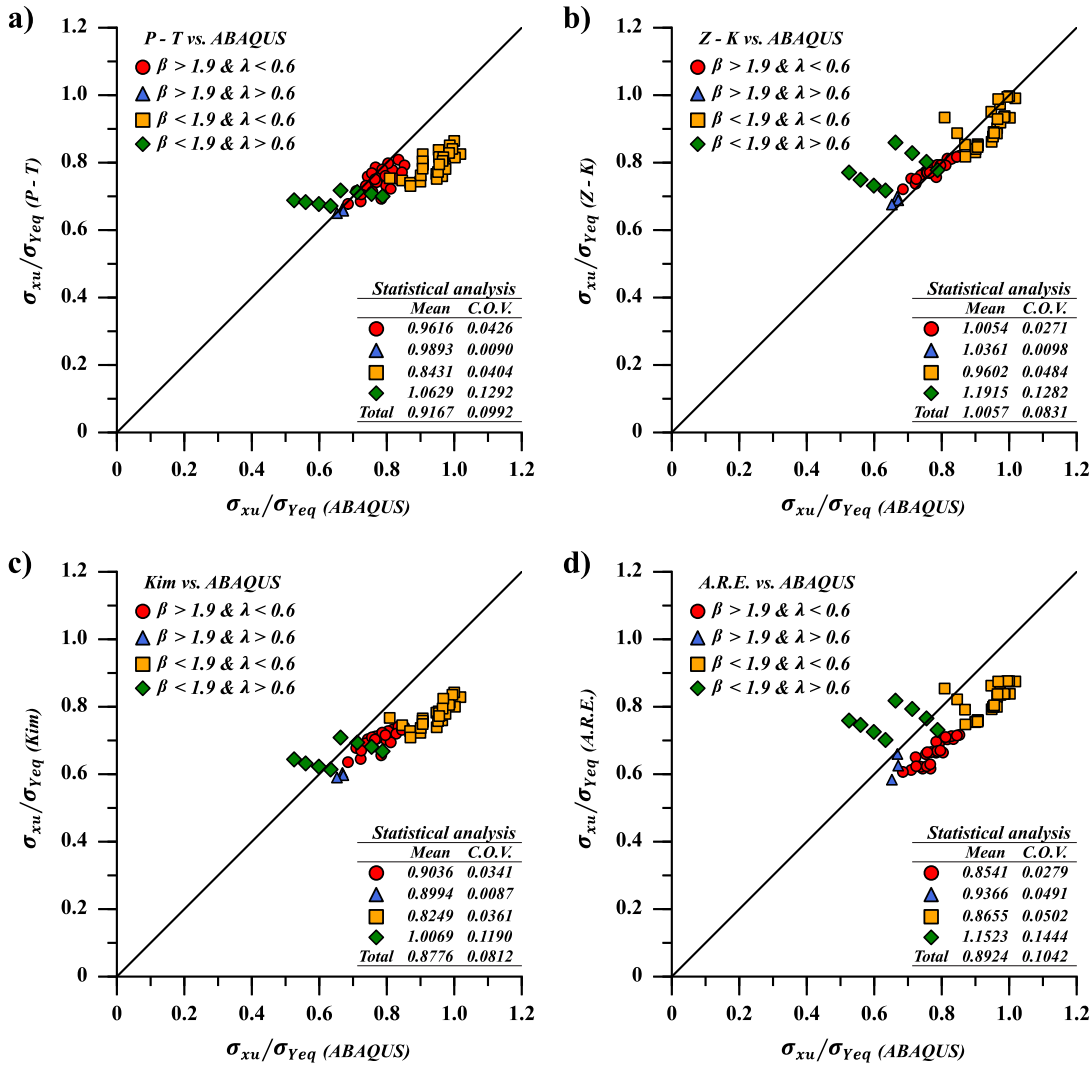

Figure 10. Comparison between NLFEM solutions and empirical formulae predictions (This figure is available in colour online).

characteristic features are shown in Figure 16, which corresponds to the variation of elastic stiffness, ultimate strain, ultimate strength and post-collapse characteristics. In addition, a worked example of the adaptable algorithm is provided in the Appendix.

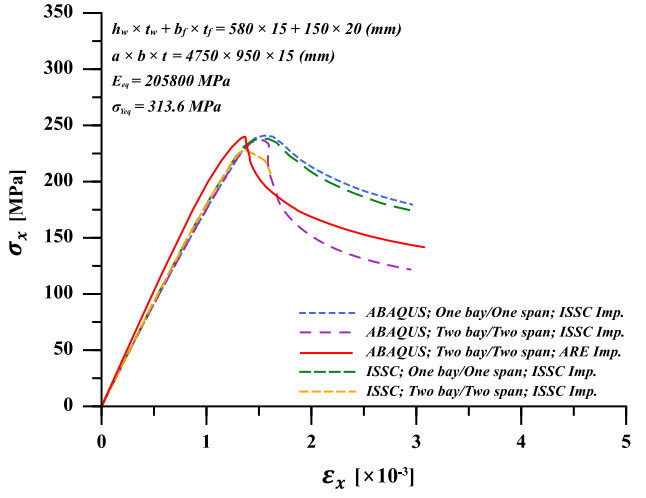

Figure 11. Comparison of load-shortening curves with benchmark study (This figure is available in colour online).

Region 1 (linear elastic response):

$$\frac{\sigma_x}{\sigma_{Yeq}} = \bar{E}_{To}\frac{\varepsilon_x}{\varepsilon_{Yeq}} \quad \text{for} \quad \frac{\varepsilon_x}{\varepsilon_{Yeq}} \le \frac{\varepsilon_{xe}}{\varepsilon_{Yeq}} \tag{10}$$

Region 2 (arc-shaped ultimate response):

$$\frac{\sigma_x}{\sigma_{Yeq}} = \frac{\sigma_{xu}}{\sigma_{Yeq}} - R + R\cos\left[-\tan^{-1}(\bar{E}_T)\right] \quad \text{for} \quad \frac{\varepsilon_{xe}}{\varepsilon_{Yeq}} < \frac{\varepsilon_x}{\varepsilon_{Yeq}} < \frac{\varepsilon_{xu}}{\varepsilon_{Yeq}} \tag{11}$$

Region 3 (post-collapse asymptotic response):

$$\frac{\sigma_x}{\sigma_{Yeq}} = C\frac{\sigma_{xu}}{\sigma_{Yeq}} + (1-C)\frac{\sigma_{xu}}{\sigma_{Yeq}}\exp\left(\frac{\varepsilon_{xu}}{\varepsilon_{Yeq}} - \frac{\varepsilon_x}{\varepsilon_{Yeq}}\right) \quad \text{for} \quad \frac{\varepsilon_x}{\varepsilon_{Yeq}} \ge \frac{\varepsilon_{xu}}{\varepsilon_{Yeq}} \tag{12}$$

$$\frac{\varepsilon_{xu}}{\varepsilon_{Yeq}} \ge \frac{\sigma_{xu}}{\sigma_{Yeq}}/\bar{E}_{To} \tag{13}$$

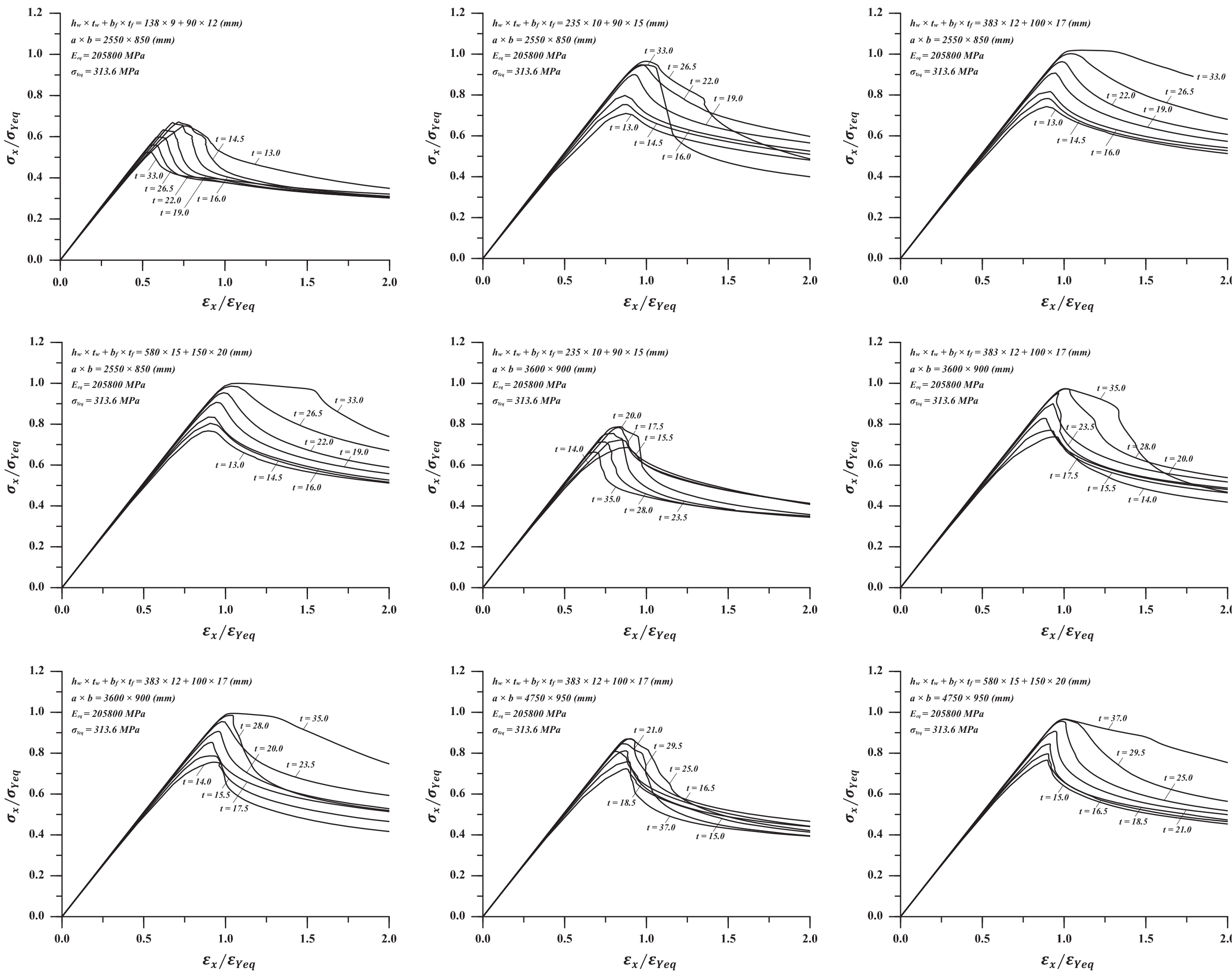

Figure 12. Load-shortening curves of stiffened panels under compression.

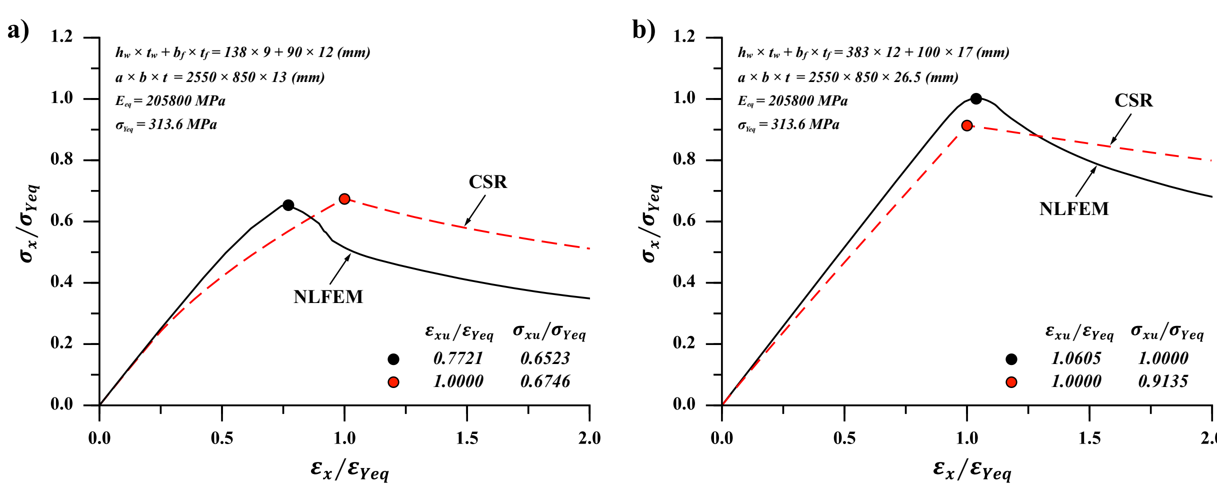

Figure 13. Comparison with CSR load-shortening curve predictions (This figure is available in colour online).

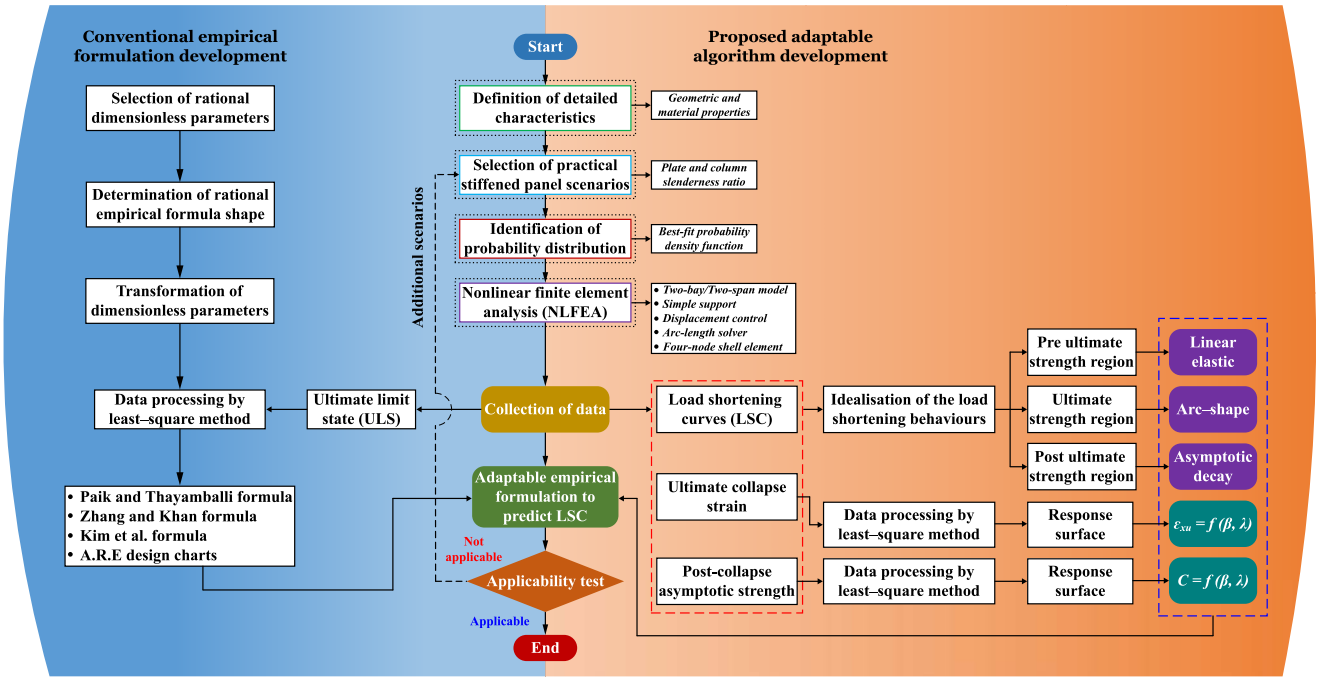

Figure 14. Procedure to develop the adaptable algorithm for predicting LSC (This figure is available in colour online).

where

$$R = \frac{\cos\left[\tan^{-1}(\bar{E}_{To})\right]\left(\bar{E}_{To}\dfrac{\varepsilon_{xu}}{\varepsilon_{Yeq}} - \dfrac{\sigma_{xu}}{\sigma_{Yeq}}\right)}{1 - \cos\left[\tan^{-1}(\bar{E}_{To})\right]} \tag{14}$$

$$\frac{\varepsilon_{xe}}{\varepsilon_{Yeq}} = \frac{\varepsilon_{xu}}{\varepsilon_{Yeq}} + R\sin\left[-\tan^{-1}(\bar{E}_{To})\right] \tag{15}$$

$\bar{E}_{To}$, Normalised initial stiffness; $\bar{E}_T$, Normalised instantaneous stiffness, incrementally varying from the initial stiffness to null at ULS.

5.2. Parameter calibration

The empirical constant C in Equation (12) dictates the asymptotic convergence of the post-collapse strength. In the present study, a provisional expression of empirical constant C is proposed, which is calibrated as the ratio between the post-collapse strength at $\varepsilon_x/\varepsilon_{Yeq} = 2.0$ and the ultimate collapse strength σ_{xu}/σ_{Yeq} (Equation (16)). A three-dimensional space illustration of the proposed expression of empirical constant C is shown in Figure 17(a).

As demonstrated in the NLFEA results, the ultimate strain of stiffened panel $\varepsilon_{xu}/\varepsilon_{Yeq}$ is not necessarily close to unity as that used by the CSR method. Hence, a provisional expression to predict the ultimate strain is introduced in the present study (Equation (17)). A three-dimensional space illustration of the proposed expression of ultimate strain is shown in Figure 17(b).

The coefficient of determination (R^2) is only around 0.4 in the calibration of the post-collapse empirical constant. This can be improved by applying more advanced data analysis techniques. With a better calibration, it is no doubt that the prediction accuracy will be improved. However, the current provisional expression is still useful for the strength calculation of commercial ships, which are less influenced by the post-collapse behaviour of the local components.

To examine the accuracy of the proposed algorithm and the provisional parameters calibration, a comparison of the area underneath the load-shortening curve predicted by NLFEM and the proposed method is completed for the case study stiffened panels listed in Table 1. As illustrated in Figure 18, the area A_1 represents the pre-ultimate strength response, while the area A_2 corresponds to the post-ultimate strength response. The results are shown in Figure 19. In terms of the pre-ultimate strength response, a close agreement is shown between the present adaptable algorithm and NLFEM. A significant deviation on the pre-ultimate strength behaviour of slender stiffened panels ($0.5 < \lambda < 0.9$) is found between the present formulation and the CSR method. This is attributed to the fact that the CSR method is embedded with unity ultimate strain, which is a large overestimation for slender stiffened panels. For the post-ultimate strength response, the present method correlates well with CSR method whilst overestimating the LSC area compared with the NLFEM. This indicates a more gradual drop of the post-

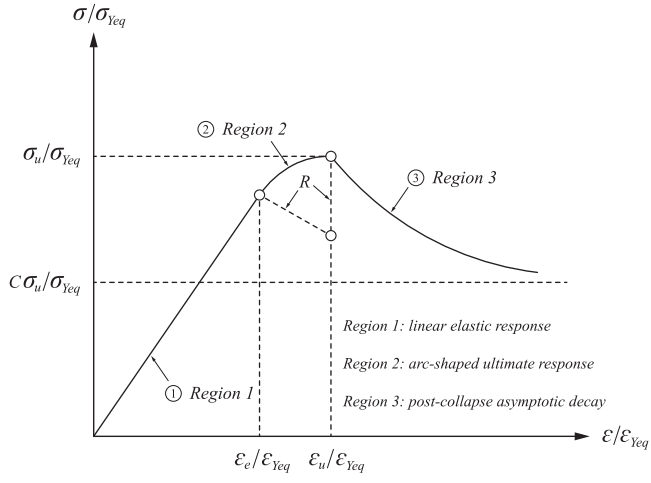

Figure 15. Graphical representation of the proposed empirical formulation.

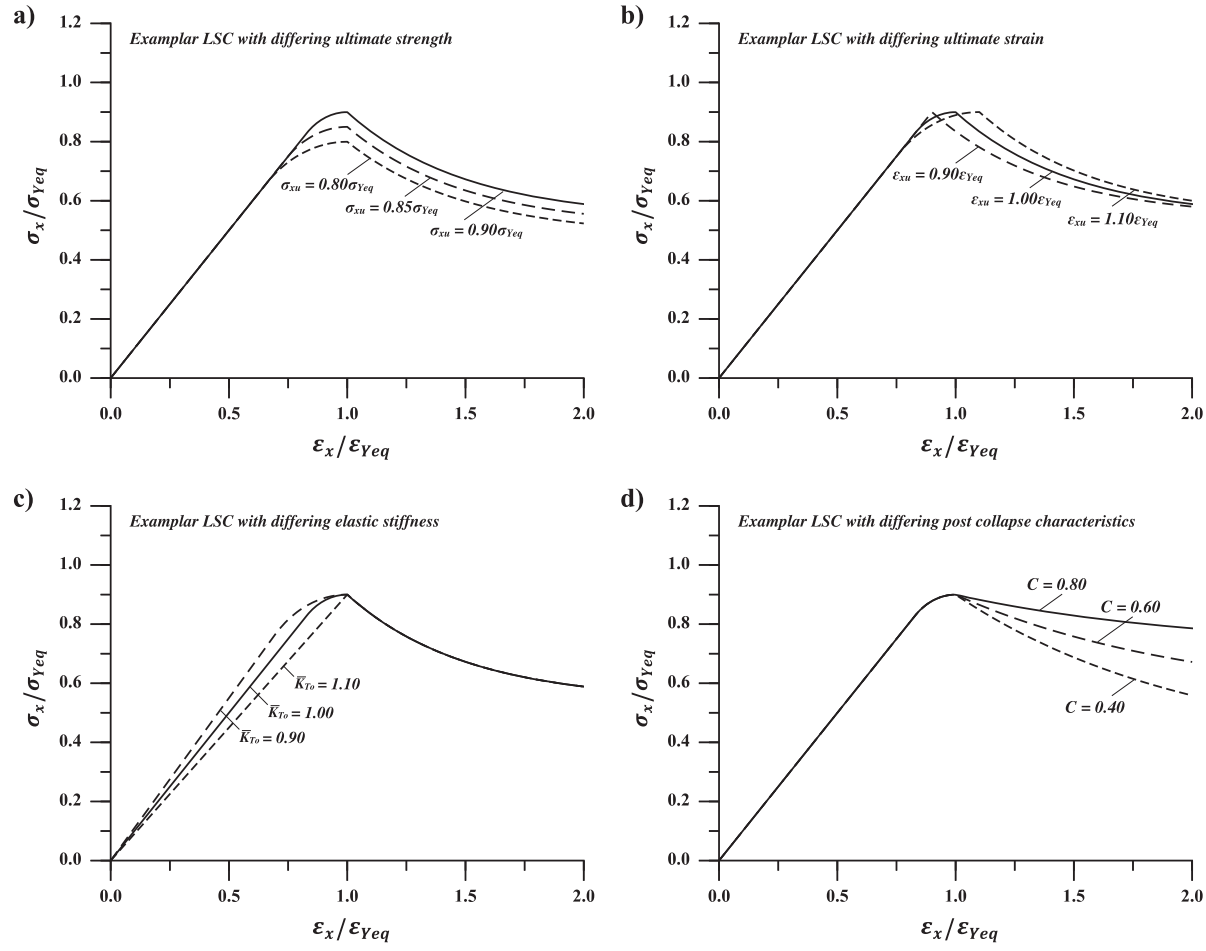

Figure 16. Example LSCs with different characteristics.

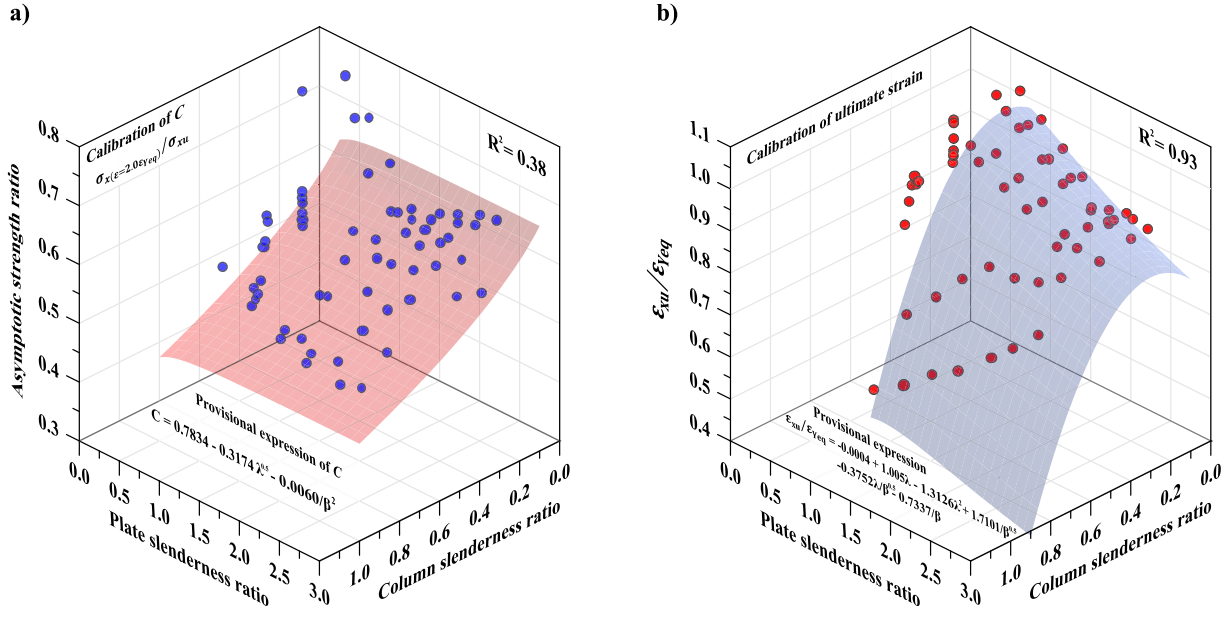

Figure 17. Parameter calibration; (a) Post-collapse strength in terms of plate slenderness ratio and column slenderness ratio; (b) Ultimate strain in terms of plate slenderness ratio and column slenderness ratio (This figure is available in colour online).

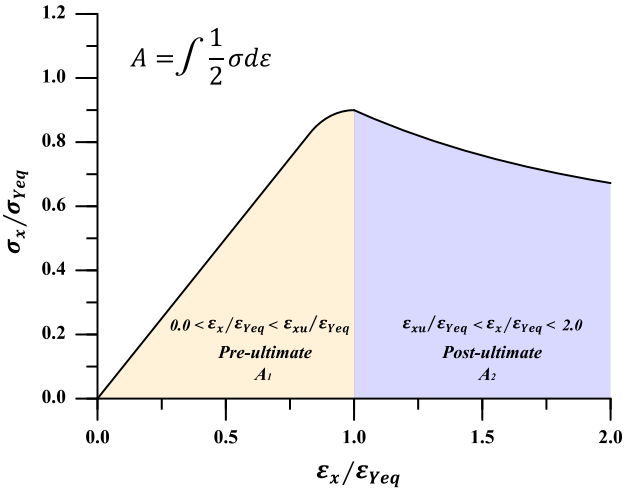

Figure 18. Schematic illustration of the area underneath a load-shortening curve (This figure is available in colour online).

ultimate strength in both present and CSR methods.

$$C = 0.7834 - 0.3174\sqrt{\lambda} - 0.0060/\beta^2 \tag{16}$$

$$\frac{\varepsilon_{xu}}{\varepsilon_{Yeq}} = -0.0004 + 1.005\lambda - 1.3126\lambda^2 + 1.7101/\sqrt{\beta} - 0.3752\lambda/\sqrt{\beta} - 0.7337/\beta \tag{17}$$

6. Application to ship hull girder progressive collapse analysis

To further demonstrate the capability of the proposed adaptable algorithm, a series of ship hull girder progressive collapse analyses are completed using the proposed formulation incorporated with the simplified progressive collapse method. As shown in Figure 20, five different ship types covering typical commercial cargo ships and a warship are analysed, namely single hull VLCC, double hull VLCC, bulk carrier, container ship and naval frigate.

The fundamental theory of the simplified progressive collapse method can be found in Smith (1977), Dow et al. (1981), Dow (1997), Benson et al. (2013b) and Li et al. (2020b). The ultimate

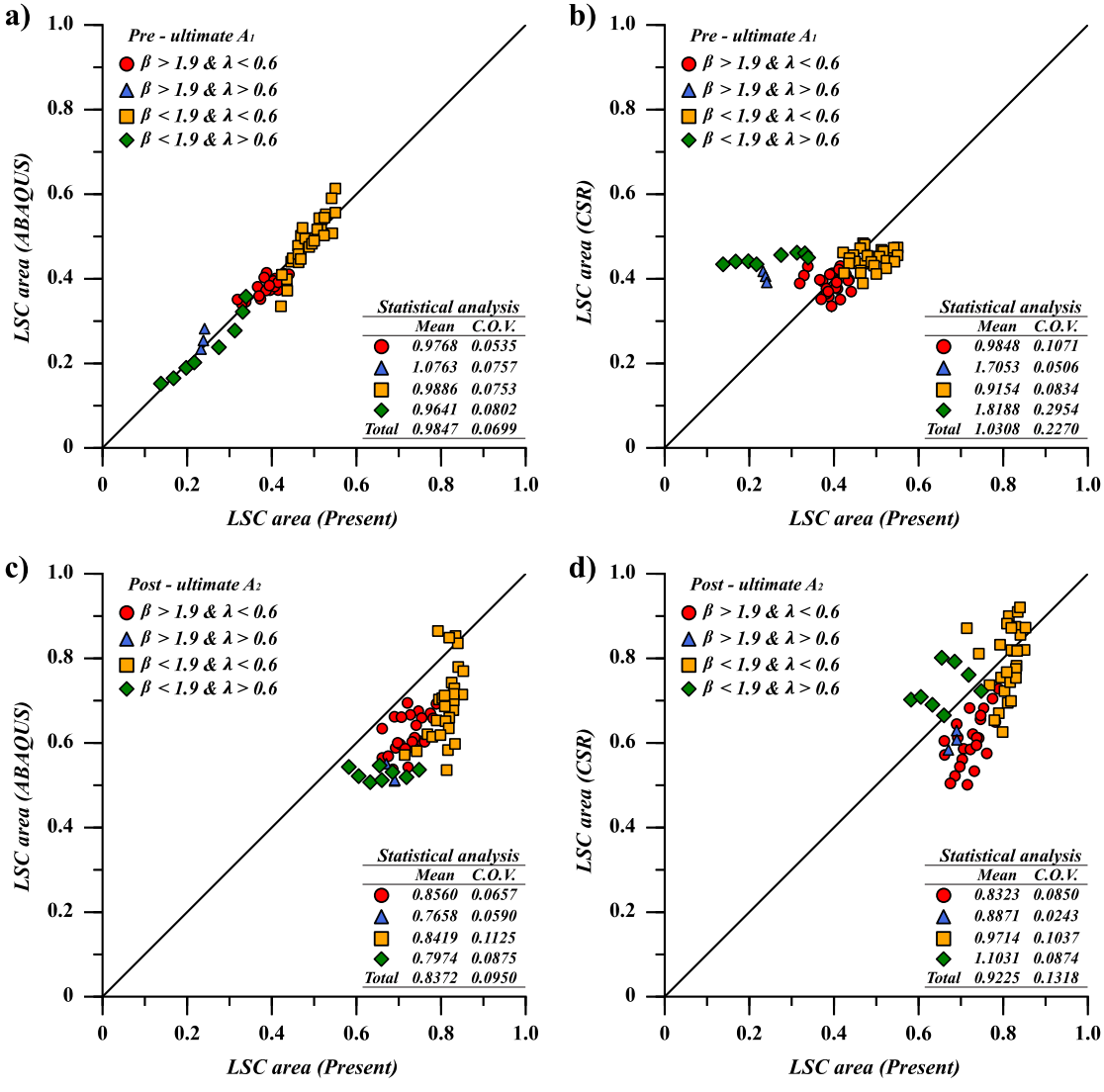

Figure 19. Comparison of the areas underneath the load-shortening curves (This figure is available in colour online).

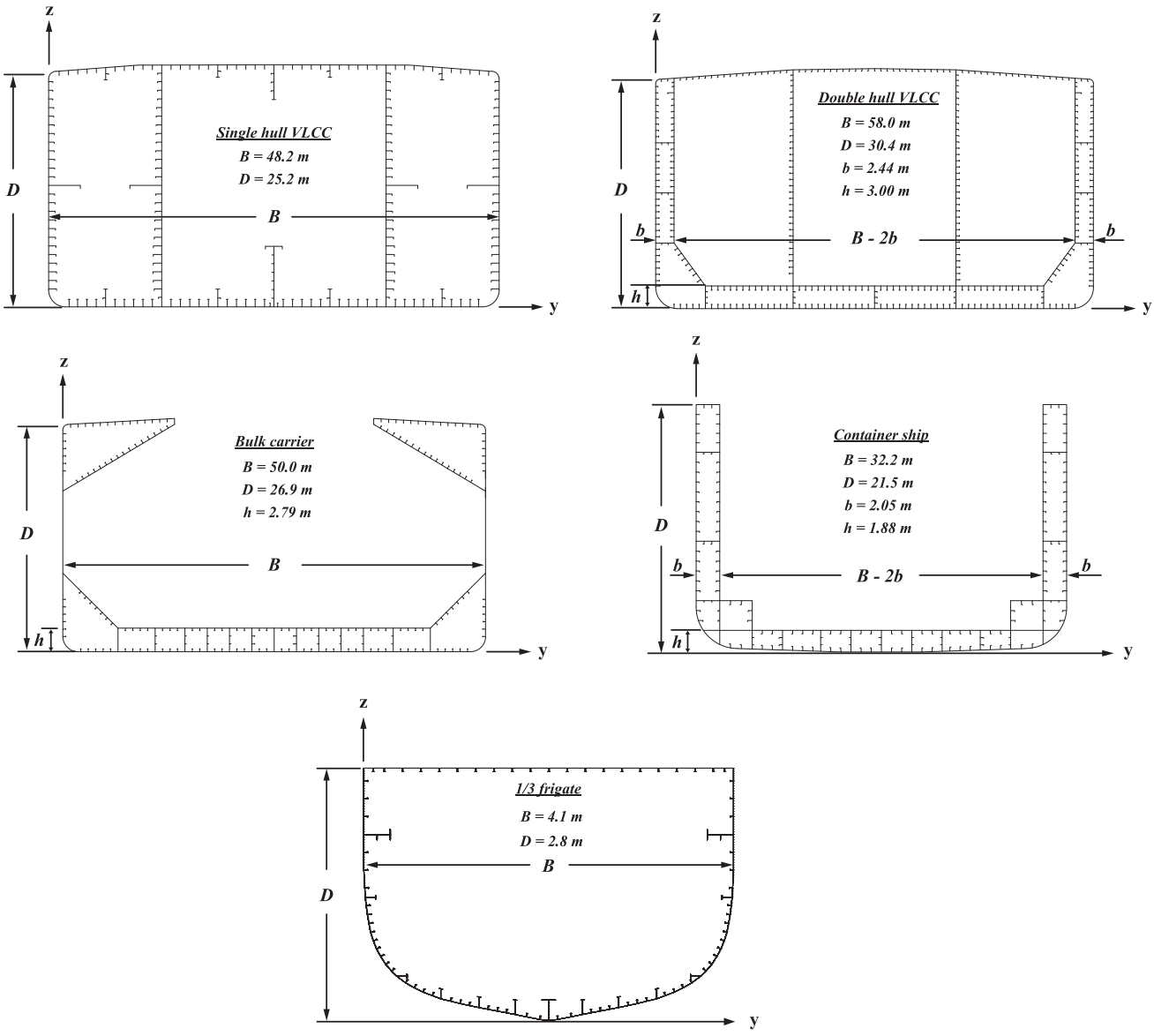

Figure 20. Selected ship hull girder cross sections.

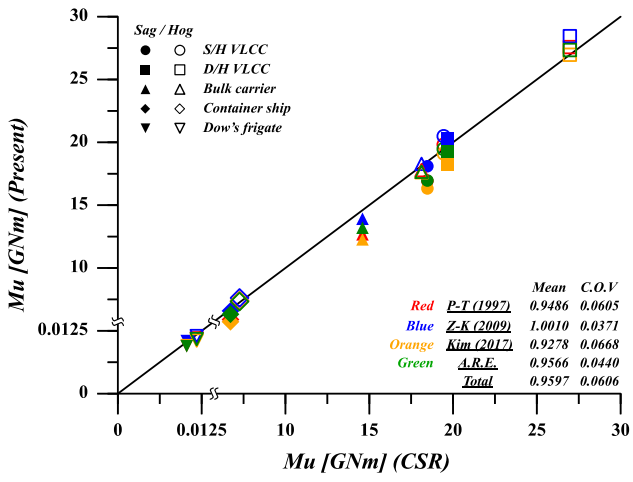

Figure 21. Comparison of the ultimate ship hull strength with CSR method (This figure is available in colour online).

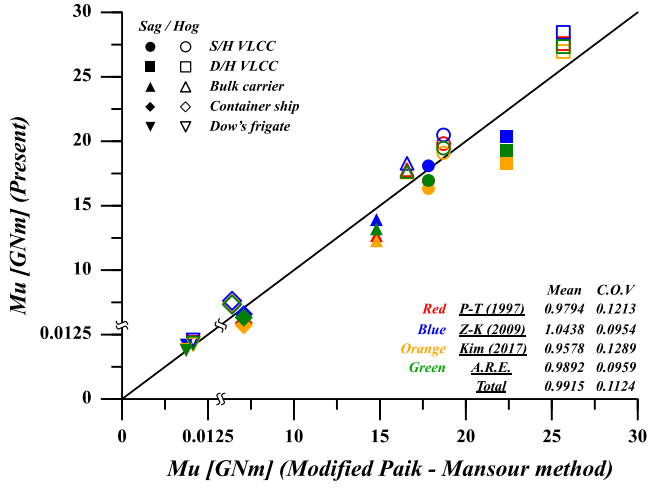

Figure 22. Comparison of the ultimate ship hull strength with modified Paik – Mansour method (This figure is available in colour online).

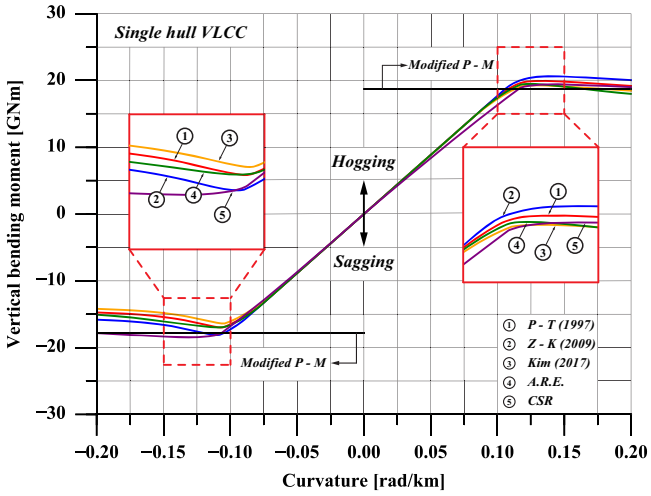

Figure 23. Comparison of bending moment/curvature relationship (Single hull VLCC) (This figure is available in colour online).

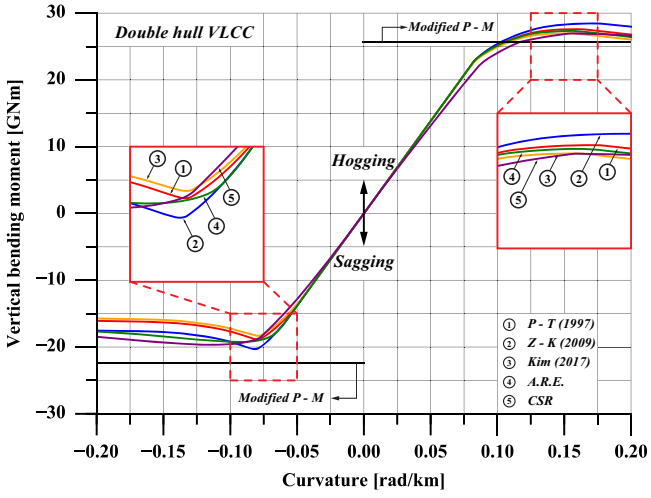

Figure 24. Comparison of bending moment/curvature relationship (Double hull VLCC) (This figure is available in colour online).

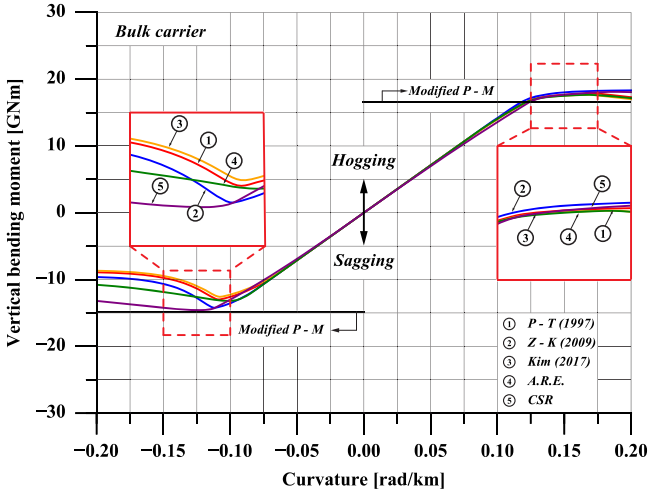

Figure 25. Comparison of bending moment/curvature relationship (Bulk carrier) (This figure is available in colour online).

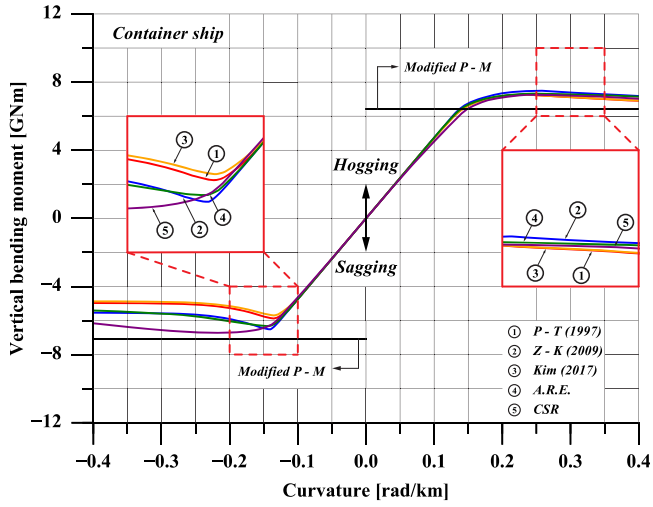

Figure 26. Comparison of bending moment/curvature relationship (Container ship) (This figure is available in colour online).

strength of stiffened panel element is predicted by four empirical formulations, namely P – T formula (1997), Z – K formula (2009), Kim formula (2017) and A.R.E. design charts. The elastic stiffness is taken as unity in accordance with the CSR method. The ultimate strain and post-collapse characteristics follows the provisional expressions given by Equations (16) and (17). Hard corner elements are considered as the nearest plate element of each intersection.

The prediction of the ultimate ship hull strength and progressive collapse behaviour are compared with the CSR method and modified Paik – Mansour method (Paik et al. 2013). Figures 21 and 22 show the comparison of ultimate ship hull strength prediction and Figures 23–27 compares the bending moment/curvature relationships. In general, a mean value of 0.96 and COV of 0.06 is obtained when comparing with CSR method, while a mean value of 0.99 and COV of 0.11 is given when comparing with the modified Paik – Mansour method. With the use of the P – T, Kim and A.R.E. formulations, there are relatively conservative predictions. Besides, the predictions in hogging are generally in closer agreement with other methods, whereas the sagging predictions have a larger scattering.

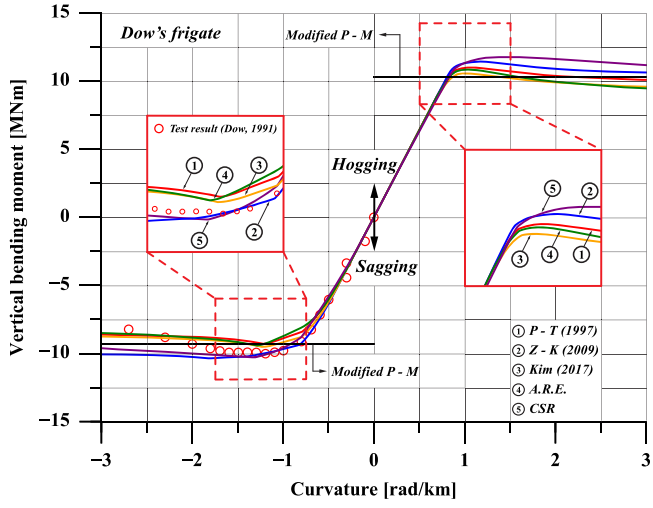

Figure 27. Comparison of bending moment/curvature relationship (Dow's frigate) (This figure is available in colour online).

7. Conclusions

This paper introduces an efficient adaptable algorithm to predict the load-shortening curve of stiffened panels under longitudinal compression. A parametric study on the nonlinear collapse behaviour of stiffened panels with various dimensions is completed using NLFEM, from which critical insights are developed for idealising the load-shortening response. The load-shortening curve predicted by the proposed approach is formed of a linear elastic initial response, arc-shape nonlinear ultimate region and an exponential post-collapse behaviour with asymptotic decay. The proposed method extends the capability of the existing empirical formulae which only can predict the ultimate compressive strength of stiffened panels. Besides, allowance is given for a convenient adaptation of the elastic stiffness, ultimate strain, ultimate strength and post-collapse characteristics.

The capability of the proposed methodology is demonstrated through an application example incorporated with the simplified progressive collapse method to predict the ultimate ship hull strength of four merchant ships and one naval vessel. A comparison is made with the CSR and modified Paik – Mansour method. The following conclusions may be made from the present study:

- The proposed algorithm is a practical and highly efficient alternative to predict the load-shortening response of stiffened panels under compression, and could be further incorporated with the simplified progressive collapse method for estimating the collapse behaviour of ship hull girders.
- The pre-ultimate strength response predicted by the present formulation closely correlates with the equivalent NLFEM prediction, but is slightly optimistic with regards to the decay of post-ultimate strength;
- The load-shortening curve prediction by the present method compares well with the CSR method in full strain range for stiffened panels with $0.1 < \lambda < 0.5$, and provides better prediction for slender stiffened panels where the CSR method has an overestimation of the ultimate strain.
- An acceptable agreement for the ship hull ultimate strength prediction further confirms the validity of the proposed formulation.

Due to its adaptability, the proposed method may be applied to evaluate the effects of specific critical features of load-shortening curves on the ultimate ship hull strength prediction, as discussed by Li et al. (2020a) with a deterministic approach and Li et al. (2021b) using a probabilistic approach.

As a future study, the effects of secondary loading and in-service degradation may be accommodated by the present approach. For instance, empirical formulae derived by Xu et al. (2018) is able to address combined compression and lateral loads. The reduction caused by a cut-out can be evaluated by the closed-form expression introduced by Paik (2007).

As the proposed algorithm is developed based on the NLFEM results, its accuracy may be subject to the NLFEM dataset. In this regard, further studies on the generation of a wider spectrum of load-shortening curve data and the application of more advanced data processing techniques are needed such as detailed regression method (Kim et al. 2019, 2020). In addition, artificial intelligence (AI) including machine learning and deep learning may also be recommended in predicting the structural capacity (Wong and Kim 2018).

Disclosure statement

No potential conflict of interest was reported by the author(s).

ORCID

Do Kyun Kim http://orcid.org/0000-0001-5735-4625

References

Anyfantis KN. 2020. Ultimate strength of stiffened panels subjected to non-uniform thrust. Int J Naval Arch Ocean Eng. 12:325–342.
Benson S. 2011. Progressive collapse assessment of lightweight ship structures. PhD Thesis, Newcastle University, Newcastle upon Tyne, UK.
Benson S, Collette MD. 2017. Finite element methods and approaches. Encyclopedia of maritime and offshore engineering. Hoboken (NJ): John Wiley & Sons.
Benson S, Downes J, Dow RS. 2011. Ultimate strength characteristics of aluminium plates for high-speed vessels. Ships Offsh Struct. 6:67–80.
Benson S, Downes J, Dow RS. 2012. An automated finite element methodology for hull girder progressive collapse analysis. In Proceeding: 13th International Marine Design Conference; Glasgow, Scotland.
Benson S, Downes J, Dow RS. 2013a. Load shortening characteristics of marine grade aluminium alloy plates in longitudinal compression. Thin Walled Struct. 70:19–32.
Benson S, Downes J, Dow RS. 2013b. Compartment level progressive collapse analysis of lightweight ship structures. Marine Struct. 31:44–62.
Benson S, Downes J, Dow RS. 2015. Overall buckling of lightweight stiffened panels using an adapted orthotropic plate method. Eng Struct. 85:107–117.
Chalmers DW. 1993. Design of ship's structures. London: HMSO.
Dow RS. 1997. Structural redundancy and damage tolerance in relation to ultimate ship hull strength. In Proceeding: Advances in Marine Structures 3, DERA, Dunfermline, Scotland.
Dow RS, Hugill RC, Clark JD, Smith CS. 1981. Evaluation of ultimate ship hull strength. In Proceeding: Extreme Load Response Symposium, Arlington, VA.
Dow RS, Smith CS. 1984. Effects of localized imperfections on compressive strength of long rectangular plates. J Constr Steel Res. 4:51–76.
Dow RS, Smith CS. 1986. FABSTRAN: a computer program for frame and beam static and transient response analysis (Nonlinear). ARE report TR86205.
Downes J, Tayyar GT, Kvan I, Choung J. 2017. A new procedure for load-shortening and -elongation data for progressive collapse method. Int J Naval Arch Ocean Eng. 9(6):705–719.
Fanourgakis SD, Samuelides M. 2021. Study of hull girder ultimate strength at elevated temperatures. Ships Offsh Struct. doi:10.1080/17445302.2021.1889897.
Faulkner DA. 1975. Review of effective plating for the analysis of stiffened plating in bending and compression. J Ship Res. 19:1–17.
Faulkner DA, Adamchak JC, Snyder GJ, Vetter MF. 1973. Synthesis of welded grillages to withstand compression and normal loads. Comp Struct. 3:221–246.
Frankland JM. 1940. The strength of ship plating under edge compression. EMM report.
Gordo JM. 2015. Effect of initial imperfections on the strength of restrained plates. J Offshore Mech Arct Eng. 137:051401.
Gordo JM, Guedes Soares C. 1996. Approximate load-shortening curves for stiffened plates under uniaxial compression. In Proceeding: Integrity of Offshore Structures 5.
IACS. 2020. Common structural rules for bulk carriers and oil tankers. International Association of Classification Societies, London, UK.
ISSC. 2000. Ultimate strength (Committee III.1), The 14th International Ship and Offshore Structures Congress (ISSC 2000), Oct 2–6, Nagasaki, Japan.
ISSC. 2012. Ultimate strength (Committee III.1), The 18th International Ship and Offshore Structures Congress (ISSC 2012), Sept 9–13, Rostock, Germany.
Kim DK, Lim HL, Kim MS, Hwang OJ, Park KS. 2017. An empirical formulation for predicting the ultimate strength of stiffened panels subjected to longitudinal compression. Ocean Eng. 140:270–280.
Kim DK, Lim HL, Yu SY. 2018a. A technical review on ultimate strength prediction of stiffened panels in axial compression. Ocean Eng. 170:392–406.
Kim DK, Lim HL, Yu SY. 2019. Ultimate strength prediction of T-bar stiffened panel under longitudinal compression by data processing: a refined empirical formulation. Ocean Eng. 192:106522.
Kim DK, Poh BY, Lee JR, Paik JK. 2018b. Ultimate strength of initially deflected plate under longitudinal compression: Part I An advanced empirical formulation. Struct Eng Mech. 68(2):247–259.
Kim DK, Young SY, Lim HL, Cho NK. 2020. Ultimate compressive strength of stiffened panel: an empirical formulation for flat-bar type. J Marine Sci Eng. 8(8):605.

Lee HH, Paik JK. 2020. Ultimate compressive strength computational modelling for stiffened plate panels with non-uniform thickness. J Mar Sci Appl. 19:658–673.
Li S, Hu ZQ, Benson S. 2019. An analytical method to predict the buckling and collapse behaviour of plates and stiffened panels under cyclic loading. Eng Struct. 199:109627.
Li S, Hu ZQ, Benson S. 2020a. The sensitivity of ultimate ship hull strength to the structural component load-shortening curve. In Proceeding: 30th International Ocean and Polar Engineering Conference (ISOPE), Shanghai, China.
Li S, Hu ZQ, Benson S. 2020b. Progressive collapse analysis of ship hull girders subjected to extreme cyclic bending. Marine Struct. 73:102803.
Li S, Kim, DK, Benson, S. 2021a. The influence of residual stress on the ultimate strength of longitudinally compressed stiffened panels. Ocean Eng. 231:108839.
Li S, Kim DK, Benson S. 2021b. A probabilistic approach to assess the computational uncertainty of ultimate strength of hull girders. Reliab Eng Syst Saf. 213:107688.
Lin YT. 1985. Ship longitudinal strength modelling. PhD thesis, University of Glasgow, Scotland.
Ozdemir M, Ergin A, Yanagihara D, Tanaka S, Yao T. 2018. A new method to estimate ultimate strength of stiffened panels under longitudinal thrust based on analytical formulas. Marine Struct. 59:510–535.
Paik JK. 2007. Ultimate strength of steel plates with a single circular hole under axial compressive loading along short edges. Ships Offsh Struct. 2:355–360.
Paik JK, Kim DK, Lee H, Shim YL. 2012. A method for analysing elastic large deflection behaviour of perfect and imperfect plates with partially rotation-restrained edges. J Offshore Mech Arct Eng. 134(2):021603.
Paik JK, Kim DK, Park DH, Kim HB, Mansour AE, Caldwell JB. 2013. Modified Paik–Mansour formula for ultimate strength calculations of ship hulls. Ships Offshore Struct. 8(3–4):245–260. https://doi.org/10.1080/17445302.2012.676247.
Paik JK, Lee DH, Noh SH, Park DK, Ringsberg JW. 2020a. Full-scale collapse testing of a steel stiffened plate structure under axial-compressive loading triggered by brittle fracture at cryogenic condition. Ships Offsh Struct. 15 (Suppl. 1):S29–S45. doi:10.1080/17445302.2020.1787930.
Paik JK, Lee DH, Noh SH, Park DK, Ringsberg JW. 2020b. Full-scale collapse testing of a steel stiffened plate structure under cyclic axial-compressive loading. Structures. 26:996–1009.
Paik JK, Lee DH, Park DK, Ringsberg JW. 2020c. Full-scale collapse testing of a steel stiffened plate structure under axial-compressive loading at a temperature of −80°C. Ships Offsh Struct. doi:10.1080/17445302.2020.1791685.
Paik JK, Seo JK. 2009a. Nonlinear finite element method models for ultimate strength analysis of steel stiffened-plate structures under combined biaxial compression and lateral pressure actions: part I: plate elements. Thin Walled Struct. 47:1008–1017.
Paik JK, Seo JK. 2009b. Nonlinear finite element method models for ultimate strength analysis of steel stiffened-plate structures under combined biaxial compression and lateral pressure actions: part II: stiffened panels. Thin Walled Struct. 47:998–1007.
Paik JK, Thayamballi A. 2003. A concise introduction to the idealised structural unit method for nonlinear analysis of large plated structures and its application. Thin Walled Structure. 41:329–355.
Paik JK, Thayamballi AK. 1997. An empirical formulation for predicting the ultimate compressive strength of stiffened panels. In Proceeding: 7th International Offshore and Polar Engineering Conference (ISOPE). Honolulu, US.
Paik JK, Thayamballi AK, Kim BJ. 2001a. Advanced ultimate strength formulations for ship plating under combined biaxial compression/tension, edge shear, and lateral pressure loads. Mar Technol. 38(1):9–25.
Paik JK, Thayamballi AK, Kim BJ. 2001b. Large deflection orthotropic plate approach to develop ultimate strength formulations for stiffened panels under combined biaxial compression/tension and lateral pressure. Thin Walled Struct. 39(3):215–246.
Paik JK, Thayamballi AK, Kim DH. 1999. An analytical method for the ultimate compressive strength and effective plating of stiffened panels. J Constr Steel Res. 49(1):43–68.
Paik JK, Thayamballi AK, Lee WH. 1998. A numerical investigation of tripping. Marine Struct. 11:159–183.
Ringsberg JW, Darie I, Nahshon K, Shilling G, Vaz MA, Benson S, Brubak L, Feng GQ, Fujikubo M, Gaiotti M, et al. 2021. The ISSC 2022 committee III.1-Ultimate strength benchmark study on the ultimate limit state analysis of a stiffened plate structure subjected to uniaxial compressive loads. Mar Struct. 79:103026.
Smith CS. 1977. Influence of local compressive failure on ultimate longitudinal strength of a ship's hull. In Proceeding: International Symposium on Practical Design of Ships and others Floating Structures, PRADS, Tokyo, Japan.
Smith CS, Anderson N, Chapman JC, Davidson PJ, Dowling PJ. 1991. Strength of stiffened plating under combined compression and lateral pressure. Trans R Instit Naval Arch. 134:131–147.
Syrigou MS, Dow RS. 2018. Strength of steel and aluminium alloy ship plating under combined shear and compression/tension. Eng Struct. 166:128–141.
Tanaka S, Yanagihara D, Yasuoka A, Harada M, Okazawa S, Fujikubo M, Yao T. 2014. Evaluation of ultimate strength of stiffened panels under longitudinal thrust. Marine Struct. 36:21–50.
Ueda Y, Rashed SMH. 1984. The idealized structural unit method and its application to deep girder structures. Comput Struct. 18:277–293.
Ueda Y, Rashed S, Paik JK. 1984. Plate and stiffened panel units of the idealized structural unit method under in-plane loading. J Soc Naval Arch Japan. 156:366–376.
Wong EWC, Kim DK. 2018. A simplified method to predict fatigue damage of TTR subjected to short-term VIV using artificial neural network. Adv Eng Softw. 126:100–109.
Xu MC, Song ZJ, Zhang BW, Pan J. 2018. Empirical formula for predicting ultimate strength of stiffened panel of ship structure under combined longitudinal compression and lateral loads. Ocean Eng. 162:161–175.
Xu MC, Yanagihara D, Fujikubo M, Guedes Soares C. 2013. Influence of boundary conditions on the collapse behaviour of stiffened panels under combined loads. Marine Struct. 34:205–255.
Yao T, Nikolov P. 1991. Progressive collapse analysis of a ship's hull under longitudinal bending (1st report). J Soc Naval Arch Japan. 170:449–461.
Yao T, Nikolov P. 1992. Progressive collapse analysis of a ship's hull under longitudinal bending (2nd report). J Soc Naval Arch Japan. 172:437–446.
Zhang S, Khan I. 2009. Buckling and ultimate capability of plates and stiffened panels in axial compression. Marine Struct. 22:791–808.

Appendix

A worked example is provided in this appendix to assist the readers with the application of the adaptable algorithm to predict the compressive load-shortening curve of a stiffened panel. The dimension and material property of the stiffened panel are given as follows:

- Attached plate: $a = 2550$ mm, $b = 850$ mm, $t = 26.5$ mm
- Stiffener: $h_w = 383$ mm, $t_w = 12$ mm, $b_f = 100$ mm, $t_f = 17$ mm
- Material property: $\sigma_{Yeq} = \sigma_{Yp} = \sigma_{Ys} = 313.6$ MPa, $E = 205800$ MPa

The non-dimensional parameter of the stiffened panel can be calculated as follows:

$$\beta = \frac{b}{t}\sqrt{\frac{\sigma_{Yp}}{E}} = 1.2521 \tag{A1}$$

$$\lambda = \frac{a}{\pi r}\sqrt{\frac{\sigma_{Yeq}}{E}} = 0.2574 \tag{A2}$$

Once the non-dimensional parameters β and λ are obtained, the ultimate compressive strength, ultimate strain and asymptotic constant of the post-collapse response can be calculated as follows:

$$\begin{aligned}\frac{\sigma_{xu}}{\sigma_{Yeq}} &= \frac{1}{0.8884 + e^{\lambda^2}} + \frac{1}{0.4121 + e^{\sqrt{\beta}}} \\ &= \frac{1}{0.8884 + e^{0.2574^2}} + \frac{1}{0.4121 + e^{\sqrt{1.2521}}} \\ &= 0.7989 \ \text{(Kim et al. formula)}\end{aligned} \tag{A3}$$

$$\begin{aligned}\frac{\varepsilon_{xu}}{\varepsilon_{Yeq}} &= -0.0004 + 1.005\lambda - 1.3126\lambda^2 \\ &\quad + 1.7101/\sqrt{\beta} - 0.3752\lambda/\sqrt{\beta} - 0.7337/\beta = -0.0004 \\ &\quad + 1.005 \times 0.2574 - 1.3126 \times 0.2574^2 + 1.7101/\sqrt{1.2521} \\ &\quad - 0.3752 \times 0.2574/\sqrt{1.2521} - 0.7337/1.2521 = 1.0273\end{aligned} \tag{A4}$$

$$\begin{aligned}C &= 0.7834 - 0.3174\sqrt{\lambda} - 0.0060/\beta^2 \\ &= 0.7834 - 0.3174 \times \sqrt{0.2574} - 0.0060/1.2521^2 = 0.6185\end{aligned} \tag{A5}$$

Following Equation (15) and assuming elastic stiffness $\bar{E}_{To} = 1.0$, the arc radius and the linear elastic limit is calculated as follows:

$$R = \frac{\cos\left[\tan^{-1}(\bar{E}_{To})\right]\left(\bar{E}_{To}\dfrac{\varepsilon_{xu}}{\varepsilon_{Yeq}} - \dfrac{\sigma_{xu}}{\sigma_{Yeq}}\right)}{1 - \cos\left[\tan^{-1}(\bar{E}_{To})\right]} = \frac{\cos\left[\tan^{-1}(1.0)\right](1.0 \times 1.0273 - 0.7989)}{1 - \cos\left[\tan^{-1}(1.0)\right]} = 0.5514 \quad \text{(A6)}$$

$$\frac{\varepsilon_{xe}}{\varepsilon_{Yeq}} = \frac{\varepsilon_{xu}}{\varepsilon_{Yeq}} + R\sin\left[-\tan^{-1}(\bar{E}_{To})\right] = 1.0273 + 0.5514 \times \sin\left[-\tan^{-1}(1.0)\right] = 0.6374 \quad \text{(A7)}$$

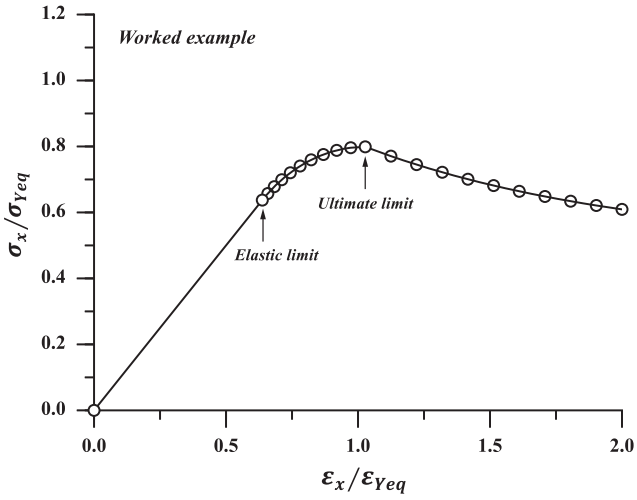

Figure A1. Illustration of the load-shortening curve worked example.

Once the above calculation is completed, the complete LSC can be derived by Equation (10)–(13). A tabular form of the predicted LSC ($0.0 \le \varepsilon_x \le 2.0\varepsilon_{xu}$) is given in Table A1 and illustrated in Figure A1, in which 10 incremental steps are used for the arc-shaped nonlinear ultimate strength response and the asymptotic post-collapse response respectively.

Table A1. Tabular form of load-shortening curve predicted by the adaptable algorithm.

Step no.	Progressive collapse regime	Normalised average strain	Normalised average stress
1	Initial linear elastic response	0.0000	0.0000
2		0.6374[a]	0.6374
3	Arc-shaped nonlinear	0.6584	0.6574
4	ultimate strength response	0.6828	0.6781
5		0.7111	0.6992
6		0.7436	0.7203
7		0.7807	0.7407
8		0.8225	0.7595
9		0.8689	0.7756
10		0.9192	0.7882
11		0.9724	0.7962
12		1.0273[b]	0.7989
13	Asymptotic post-collapse	1.1246	0.7707
14	response	1.2218	0.7450
15		1.3191	0.7218
16		1.4164	0.7007
17		1.5137	0.6815
18		1.6109	0.6641
19		1.7082	0.6484
20		1.8055	0.6341
21		1.9027	0.6211
22		2.0000	0.6093

[a]Linear elastic limit.
[b]Ultimate strain.